

Large differences of highly oxygenated organic molecules (HOMs) and low volatile species in SOA formed from ozonolysis of β -pinene and limonene

Dandan Liu^{1#}, Yun Zhang^{2,3#}, Shujun Zhong¹, Shuang Chen¹, Qiaorong Xie¹, Donghuan Zhang¹, Qiang Zhang¹, Wei Hu¹, Junjun Deng¹, Libin Wu¹, Chao Ma¹, Haijie Tong^{4,5}, Pingqing Fu¹

¹Institute of Surface-Earth System Science, School of Earth System Science, Tianjin University, Tianjin 300072, China

²Innovation Center of Pesticide Research, Department of Applied Chemistry, College of Science, China Agricultural University, Beijing 100193, China

³Institute of Chemistry, Johannes Gutenberg University, Mainz 55128, Germany

⁴Multiphase Chemistry Department, Max Planck Institute for Chemistry, Mainz 55128, Germany

⁵Institute of Surface Science, Helmholtz-Zentrum Hereon, Geesthacht 21502, Germany

These authors contributed to this study equally.

Correspondence to: Haijie Tong (haijie.tong@hereon.de); Pingqing Fu (fupingqing@tju.edu.cn).

Abstract. Secondary organic aerosols (SOA) play a key role in climate change and public health. However, the oxidation state and volatility of SOA are still not well understood. Here, we investigated the highly oxygenated organic molecules (HOMs) in SOA formed from ozonolysis of β -pinene and limonene. ~~Extraction of SOA from particulate matter on filter samples to analysis water-soluble organic matter.~~ Fourier transform ion cyclotron resonance mass spectrometry (FT-ICR MS) was used to characterize HOMs ~~in aerosol filter samples~~, and a scanning mobility particle sizer (SMPS) was used to measure the concentration and size distribution of SOA particles. ~~The relative abundance of HOMs (i.e., abundance of HOMs in limonene SOA ratio of summed mass spectrometry peak intensity sum of HOMs to totally identified organic compounds) in limonene SOA was 5–13%–14~20%~~, higher than in β -pinene SOA (3~13%), exhibiting different trends with increasing ozone concentrations. β -pinene oxidation-derived HOMs prefer to ~~stabilize~~ ~~saturnate~~ ~~be constant~~ at high ozone concentration, accompanied by substantial formation of ultra-low-volatility organic compounds (ULVOCs). ~~Limonene~~ ~~limonene~~-oxidation-derived HOMs prefer to ~~saturnate~~ ~~stabilize~~ at moderate ozone concentrations, with semi-, low-, and extremely low-volatility organic compounds (SVOCs, LOVCs, and ELVOCs) play a major role. Combined experimental evidence and theoretical analysis indicate that oxygen-increasing-based peroxy radical chemistry is a plausible mechanism for the formation of ~~oxygenated organic~~ compounds with 10 carbon atoms. Our findings show that HOMs and low volatile species in β -pinene and limonene SOA are largely different. The ozone concentration-driven SOA formation and evolution mechanism ~~foref~~ ~~monoterpenes~~ ~~monoterpenes-derived SOA~~ is suggested to be considered in future climate or exposure risk models, which may enable more accurate air quality prediction and management.

Formatted: Font color: Blue

Formatted: Font color: Blue

Formatted: Font color: Blue

Formatted: Font color: Blue

Formatted: Font color: Blue

Formatted: Font color: Blue

Formatted: Font color: Blue

Formatted: Font color: Blue

Formatted: Font color: Blue

Formatted: Font color: Text 1

Formatted: Font color: Text 1

30 1 Introduction

Secondary organic aerosols (SOA) are key component of airborne particulate matter, which play a crucial role in air quality, ~~public health, climate, hydrological cycle, and public health hydrological cycle~~ (Laden et al., 2006; Cohen et al., 2017; Kourtchev et al., 2016; Jokinen et al., 2015; Tröstl et al., 2016; Perraud et al., 2012; Ramanathan et al., 2001; Noziere et al., 2015). ~~The SOA formed from oxidation of biogenic source volatile organic compounds (BVOCs) such as Monoterpenes monoterpenes (C₁₀H₁₆) are a class of biogenic source volatile organic compounds (BVOCs) acting as important precursors of SOA contribute a significant fraction of mass to total aerosols~~ (Kanakidou et al., 2005; Hallquist et al., 2009; Ehn et al., 2012; Fu et al., 2009). ~~However, biogenic SOA formation is a complex multiphase process (Shrivastava et al., 2017), in which biogenic SOA can be formed via the peroxy radical (RO₂) chemistry of BVOCs initiated by ozone (O₃), nitrate radicals (NO₃), and hydroxyl radicals (OH), etc. (Griffin et al., 1999; Hallquist et al., 2009; Jokinen et al., 2014; Shrivastava et al., 2017; Chen et al., 2011; Liu et al., 2016; Wang et al., 2023) (Shrivastava et al., 2017). The formation mechanism of SOA especially biogenic SOA is still largely unknown. Deep insights into understanding of biogenic SOA formation and evolution at a molecular level will facilitate the clarification of SOA's impacts on climate change and human health (Hallquist et al., 2009; Shah et al., 2019).~~

~~β -pinene and limonene are typical and important biogenic precursors that are released approximately 30.3 Tg yr⁻¹ globally (Guenther et al., 2012). The molecular composition of these two compounds contains the same number of carbon atoms, hydrogen atoms, and double bond equivalents (DBE). However, β -pinene has a bicyclic structure with an exocyclic double bond, whereas limonene has a monocyclic structure with an exocyclic double bond and an endocyclic double bond, which is more reactive than the former one (Gallimore et al., 2017; Kenseth et al., 2018). Ozonolysis of limonene takes place on the endocyclic double bond (predominantly) as well as on the exocyclic double bond, while endocyclic double bond is the only reactive site for β -pinene oxidation. Therefore, limonene exhibits greater reactivity toward ozone, resulting in a higher SOA yield than β -pinene (Tomaz et al., 2021; Bianchi et al., 2019). Laboratory simulations also confirmed that the molar yield of HOMs by β -pinene ozonolysis is much lower than that of limonene ozonolysis (Ehn et al., 2014; Jokinen et al., 2015) (Lee et al., 2006; Jokinen et al., 2015a). Thus, the structure-dependent reactivity of biogenic precursors is an important factor driving their role in atmospheric chemistry. Beyond this, the effects of different atmospheric oxidants on the SOA chemistry of biogenic precursors should also be clarified.~~

~~Gas phase ozonolysis, hydroxyl radical (OH) chemistry, and nitrate radical (NO₃) oxidation etc. have been found as effective formation pathways for biogenic SOA (Kroll and Seinfeld, 2008; Kirkby et al., 2016), with the partition of low volatile organic compounds on exiting seed particles or homogeneous nucleation as key particle formation pathways (Donahue et al., 2012; Saukko et al., 2012). The relative contributions of different these competitive BVOCs oxidation pathway processes to atmospheric particulate matter pollution depend vary as on the nature of the parent VOC and atmospheric conditions (Mahilang et al., 2021). The yield of monoterpene SOA also strongly depends on oxidant types and concentrations. For instance, Zhao et al. found that the SOA yield of ozone degradation of monoterpenes ozonolysis was higher than that of OH oxidation (Zhao et al., 2015).~~

Formatted: Font color: Blue

Formatted: Font color: Blue

Formatted: Font color: Blue

Formatted: Font color: Blue

Formatted: Font color: Blue

Formatted: Font color: Blue

Formatted: Font color: Blue

Formatted: Font color: Blue

Formatted: Font color: Blue

Formatted: Font color: Blue

Formatted: Font color: Blue

Formatted: Font color: Blue

Formatted: Font color: Blue

Formatted: Font color: Blue

Formatted: Font color: Blue

Formatted: Pattern: Clear

Formatted: Font color: Blue

Formatted: Font color: Blue, Superscript

Formatted: Font color: Blue

Formatted: Font color: Blue

Waring et al. also found that the number concentration of α -terpineol SOA was higher than limonene SOA at higher but not at lower concentrations of ozone (Waring et al., 2011). Moreover, the oxidant (e.g., O_3 or 'OH)-dependent SOA yield difference of β -pinene has a different magnitude from limonene (Jokinen et al., 2015; Mutzel et al., 2016). To unravel the underlying multiphase chemistry of these complicate processes, the composition and particle composition-volatility and volatility of biogenic SOA particles should be addressed. However, our current understanding of the mechanisms of SOA formation is limited and the impact of biogenic emissions on global climate remains uncertain (Hallquist et al., 2009; Shah et al., 2019). Previous studies indicate that biogenic SOA comprise thousands of organic compounds, which exhibit a wide range of volatilities (Donahue et al., 2012; Ehn et al., 2014; Simon et al., 2020). Based on grouping the estimated effective saturation mass concentrations C_0 (Schervish and Donahue, 2020), the volatility of organic aerosols has been categorized into volatile organic compounds (VOCs, $3 \times 10^{-9} < C_0 < 3 \times 10^6 < 3 \times 10^{-5} \mu\text{g m}^{-3}$), intermediate volatility OC (IVOCs, $3 \times 10^{-4} < C_0 < 3 \times 10^{-6} \mu\text{g m}^{-3}$), semivolatile OC (SVOCs, $0.3 < C_0 < 300 \mu\text{g m}^{-3}$), low-volatile OC (LVOCs, $3 \times 10^{-5} < C_0 < 0.3 \mu\text{g m}^{-3}$), extremely low-volatile OC (ELVOCs, $3 \times 10^{-9} < C_0 < 3 \times 10^{-5} \mu\text{g m}^{-3}$), and ultralow-volatile OC (ULVOCs, $C_0 < 3 \times 10^{-9} \mu\text{g m}^{-3}$), respectively (Hallquist et al., 2009; Simon et al., 2020). Iyer et al. suggested that after a single oxidant attack, BVOCs can be oxidized to low-volatility species on sub-second timescales, which consequently undergo decomposition or bear new particle formation (Iyer et al., 2021). Recent studies also showed that oxidation of BVOCs can produce large amounts of SOA particles via the nucleation of ULVOCs with the absence of sulfuric acid (Kirkby et al., 2016; Guo et al., 2022). As a result, the irreversible distribution of (extremely) low volatile oligomer on the aerosol surface is expected to be enhanced (Zhang et al., 2017). Beyond this, ELVOCs have been found playing a crucial role in the generation of atmospheric cloud condensation nuclei (Kerminen et al., 2012) and new particle formation in most continental regions (Jokinen et al., 2015) (Jokinen et al., 2015a). To disclose the role of different VOC subgroups in the formation and environmental impacts of SOA, it is of critical importance to chemically resolve their oxidation state and linkage with SOA evolution processes. Highly oxygenated organic molecules (HOMs) have been found as a class of O-enriched multifunctional organic compounds (Tröstl et al., 2016). These HOMs frequently have a variety of redox functionalities (Zhang et al., 2017; Kirkby et al., 2016), playing an important role in the early growth of atmospheric organic aerosols (Ehn et al., 2014; Wang et al., 2020), and are closely associated with the formation of aqueous radicals (Tong et al., 2019) (Ehn et al., 2014; Wang et al., 2020). Ehn et al. found that HOMs in Hyytiälä's atmosphere, laboratory-generated α - and β -pinene SOA always have a $O/C > 0.7$ (Ehn et al., 2012). Tröstl et al. suggested that α -pinene SOA-contained HOMs can be defined as $C_xH_yO_z$ with $x = 8 \sim 10$, $y = 12 \sim 16$ and $z \geq 6$ for monomer and $C_xH_yO_z$ with $x = 17 \sim 20$, $y = 26 \sim 32$ and $z \geq 8$ for dimer (Tröstl et al., 2016) (Tröstl et al., 2016b). Tu et al. defined HOMs in fresh and aged biogenic (α -pinene, β -pinene, and limonene) SOA as assigned formulas having either $O/C \geq 0.6$ or carbon oxidation states $OS_C \geq 0$, which were also categorized into highly oxygenated and highly oxidized HOMs ($O/C \geq 0.6$ and $OS_C \geq 0$), highly oxygenated but less oxidized HOMs ($O/C \geq 0.6$ but $OS_C < 0$), and highly oxidized HOMs with a moderate level of oxygenation ($OS_C \geq 0$ but $H/C < 1.2$) for exploring the relative importance of oxygen content versus oxidation state (Kroll et al., 2011; Tu et al., 2016). Tröstl et al. $C_xH_yO_z$ with $x = 8 \sim 10$, $y = 12 \sim 16$ and $z \geq 6$ $C_xH_yO_z$ with $x = 17 \sim 20$, $y = 26 \sim 32$ and $z \geq 8$ (Tröstl et al., 2016) Further study showed that monoterpene SOA-contained

Formatted

Formatted: Font color: Blue

Formatted: Font color: Blue

Formatted

Formatted

Formatted

Formatted: Font color: Blue

Formatted

Formatted

Formatted

Formatted: Font color: Blue

Formatted

HOMs mainly composed of ELVOCs, LVOCs, and a small proportion of SVOCs (Li et al., 2019). (Zhang et al., 2017; Kirkby et al., 2016b) Beyond the biogenic SOA, aromatic SOA and aged soot particles have also been found containing substantial fraction of HOMs (Molteni et al., 2018; Li et al., 2022). Respect to the formation mechanism of HOMs, autoxidation has been suggested to be an important pathway (Crouse et al., 2013; Rissanen et al., 2014). For instance, peroxy radicals (RO₂) can undergo an intramolecular hydrogen atom shift (H-shift) to form a hydroperoxide functionality (HOO-) and an alkyl radical (RO), and then molecular oxygen rapidly attaches to form a new more oxidized RO₂ radical, and be repeated several times to form HOMs (Bianchi et al., 2019). Given the different yield, lifetime, and reactivity of HOMs in different types of SOA (Ehn et al., 2014; Jokinen et al., 2015; Pullinen et al., 2020; Shen et al., 2021; Guo et al., 2022), it is necessary to differentiate the compositional characteristics of HOMs in different types of SOA.

In short, BVOCs in the atmosphere undergo diverse oxidation chemistry pathways. Previous studies have shown the complicated synergy of BVOCs and atmospheric oxidants such as ozone in atmospheric processing (Wu et al., 2020a, b) (Rohr et al., 2003; Pathak et al., 2012) (Wu et al., 2020b) (Rohr et al., 2003; Pathak et al., 2012; Wu et al., 2020). However, the compositional response of biogenic SOA especially the particulate HOMs is largely unknown. Given the continued even worsened ozone pollution scenarios widely (Li et al., 2023), a better understanding of the interconnections among ozone concentrations, BVOCs types, and HOM distributions will be extremely important. Bianchi et al. (2019) have described the relation between HOMs and the volatility classes, which are ULVOCs/ELVOCs, low volatile organic compounds (LVOCs), and semi-volatile organic compounds (SVOCs). Among them, HOMs are an important component of (E)LVOCs, and a small proportion may be volatile enough to be classified as SVOCs (Li et al., 2019). The ELVOCs in this paper refer to formula for calculating the volatility of organic aerosols based on effective saturation mass concentrations ($3 \times 10^{-9} < C_{\mu} < 3 \times 10^{-5} \mu\text{g}\cdot\text{m}^{-3}$) according to Schervish and Donahue (Schervish and Donahue, 2020), while the HOMs are determined on the basis of the oxygen number in a formula (see section 2.4).

Recent research has shown that after a single oxidant attack, the BVOCs can be oxidized to low volatility aerosol precursors on sub-second timescales, which consequently undergo decomposition or participate in new particle formation (Iyer et al., 2021). SOA are composed of thousands of organic compounds exhibiting contains contain organic species with a wide range of volatility, which has a strong temperature dependence a wide range of volatile characteristics volatilities, such as semi-low-, and extremely low-volatile organic compounds (SVOCs, LVOCs, and ELVOCs) etc. (Hallquist et al., 2009; Simon et al., 2020). In contrast, ambient species are thought to consist mainly of low-volatile species, potentially reducing the atmospheric relevance of laboratory-generated SOA SOA species in the ambient atmosphere are thought to consist mainly of low-volatile species, potentially overestimating the contribution of laboratory SOA to environmental SOA (Kim and Paulson, 2013). As SOA functionalization and oxygenated compounds increase, the vapor pressure decreases and gaseous compounds condense on existing particles or nucleate to form new compound particles The reduced volatility of the gas phase compound is accompanied by a reduction in vapour pressure, which may condense on existing particles or form new ones (Donahue et

Formatted: Font color: Blue

Formatted: Font color: Blue

Formatted: Font color: Blue

Formatted: Font color: Blue

Formatted: Font color: Blue

Formatted: Font color: Blue

Formatted: Font color: Blue

Formatted: Font color: Blue

Formatted: Font color: Blue

Formatted: Font color: Blue

Formatted: Font color: Blue

Formatted: Font color: Blue

Formatted: Font color: Blue

Formatted: Font color: Blue

Formatted: Font color: Blue

Formatted: Font color: Blue

Formatted: Font color: Blue

Formatted: Font color: Blue

Formatted: Font color: Blue

Formatted: Font color: Blue

Formatted: Font color: Blue

al., 2012; Saukko et al., 2012). Ozonolysis is the most effective formation pathway of semi-, low-, or extremely low-volatile organic compounds (ELVOCs) that contribute significantly to SOA formation (Kroll and Seinfeld, 2008; Kirkby et al., 2016a). Beyond this, recent experimental results have also shown that BVOCs can produce large amounts of aerosol particles via the nucleation of ultra-low-volatility organic compounds (ULVOCs) with the formation of ultra-low-volatility organic compounds (ULVOCs) even in the absence of sulfuric acid (Kirkby et al., 2016a; Guo et al., 2022). In particular, as a result of the irreversible distribution of (extremely) low volatility of the oligomer, it is expected that its irreversible distribution on the aerosol surface is expected to be enhanced (Zhang et al., 2017). Moreover, ELVOCs play a crucial role in the generation of atmospheric cloud condensation nuclei (Kerminen et al., 2012). ELVOCs are mainly derived from monoterpene oxidation and enhance new particle formation in most continental regions (Jokinen et al., 2015a).

And a key starting point for the formation and growth of new particles is the formation of highly oxidized organic molecules (HOMs), which are a class of organic compounds with a variety of functionalities and a large amount of oxygen atoms (Ehn et al., 2014).

HOMs with high oxygen-containing but low oxidation state highly oxygenated but less oxidized should determine the oxidation potential of ambient fine particles and laboratory-generated SOA (Tu et al., 2016; Tong et al., 2019). HOMs refer to compounds formed via the process of autoxidation in which a RO_2 peroxy radical (RO_2) undergoes an intramolecular hydrogen atom shift (H-shift) to form a hydroperoxide functionality (HOO) and an alkyl radical (RO), and then molecular oxygen rapidly attaches to form a new more oxidized RO_2 radical, and this process is repeated several times (Bianchi et al., 2019).

Recent research has shown that after a single oxidant attack, the BVOCs can be oxidized to low-volatility aerosol precursors on sub-second timescales, which are then decomposed into aerosols, and even participate in the formation of new particles (Iyer et al., 2021). Laboratory studies of HOMs observed by ozonolysis of monoterpenes are closely corresponded to observations from boreal forests (Ehn et al., 2012; Ehn et al., 2014). Bianchi et al. (2019) have described the relation between HOMs and the volatility classes. The classes are ULVOCs/ELVOCs, low-volatile organic compounds (LVOCs), and semi-volatile organic compounds (SVOCs). Among them, HOMs are an important component of (E)LVOCs, and a small part proportion may be volatile enough to be classified as SVOCs (Li et al., 2019). The ELVOCs in this paper refer to formula for calculating the volatility of organic aerosols based on effective saturation mass concentrations ($3 \times 10^{-9} < C_o < 3 \times 10^{-5} \mu\text{g m}^{-3}$) according to Schervish and Donahue (Schervish and Donahue, 2020), while the HOMs are determined on the basis of the oxygen number in a formula (see section 2.4).

Due to their low volatility, monoterpene HOMs can provide nucleation conditions may nucleate for the play important role in the early growth of nanoparticles (Tröstl et al., 2016). The more abundant atmospheric β -pinene and limonene as more abundant precursors to atmospheric emissions, which are used in this study, are released approximately 30.3 Tg yr^{-1} globally (Guenther et al., 2012). The molecules of β -pinene and limonene have the same number of carbon and hydrogen atoms as well as double bond equivalents (DBE). β -pinene as the second most abundant VOC has a bicyclic structure with an exocyclic double bond as the second most abundant VOC and limonene has a monocyclic structure with an exocyclic and an endocyclic double bond, though the endocyclic double bond is more reactive (Gallimore et al., 2017; Kenseth et al., 2018b). Thus, even

165 at low concentrations in the atmosphere, limonene has a high potential for SOA formation due to its greater reactivity toward
ozone (Tomaz et al., 2021; Bianchi et al., 2019). For limonene, the attack of ozone takes place predominantly on the endocyclic
double bond, and for β -pinene, it is the only reactive site. Laboratory studies have shown that the molar yield of HOMs by β -
pinene ozonolysis is much lower than that of limonene ozonolysis (Ehn et al., 2014; Jokinen et al., 2015a). The ozone
chemistry-based SOA formation potential of these two compounds (limonene > β -pinene) is described in other literature (Lee
170 et al., 2006; Jokinen et al., 2015a). Notably, β -pinene and limonene showed opposite trends in SOA formation potential under
the condition of \cdot OH oxidation (Jokinen et al., 2015a; Mutzel et al., 2016). This reflects that BVOCs in the atmosphere exhibit
diverse oxidation chemistry and have different product responses.

The nucleation rate yield of monoterpene SOA is largely dependent on oxidant types and concentrations. For instance, Zhao
et al. found that the SOA yield of ozone degradation of monoterpenes was higher than that of \cdot OH oxidation (Zhao et al., 2015).
175 Moreover, the initial nucleation of limonene SOA was found to be maximum at low ozone concentrations, while the opposite
behavior was observed at high ozone concentrations. Previous studies found that the number concentration of α -terpineol SOA
was higher than limonene SOA at high concentrations of ozone, while the the number concentration of limonene SOA was
higher than α -terpineol SOA at low concentrations of ozone (Waring et al., 2011). In addition, high BVOC emissions has been
found to increase surface ozone and SOA levels in China (Wu et al., 2020a). Moreover, laboratory studies often use high
180 concentrations of ozone to reduce the loss of semi-volatile and low volatile vapors to the walls of the chamber (Pathak et al.,
2008). Thus, deepened the understanding of ozone concentration-dependent SOA and HOM formation mechanisms, it is
necessary to study the effect of will also enable more accurate, reproducible, and reliable chamber studies ozone concentration
on the molecular composition of monoterpene SOA particularly the volatility and oxidation state driven constituents (e.g.,
HOMs and ELVOCs).

185 The aim of this study was to analyze the influence of ozone concentration on the chemical composition of SOA formed from
 β -pinene and limonene ozonolysis. The experiments were carried out in a flow tube reactor at three different gradient ozone
concentrations. Then Fourier transform ion cyclotron resonance mass spectrometer equipped with a 7 Tesla superconducting
magnet (7T FT-ICR MS) was used to study obtain the molecular composition and indirectly infer formation reaction mechanism
of polar SOA organic extracted with ultrapure Milli-Q water. These efforts provide highly accurate molecular mass
190 measurements of organic compounds to clearly assign molecular formulas including carbon, hydrogen, and oxygen up to 850
Da, which enables the to explore the differentiation ee of of particulate HOMs originating from β -pinene and limonene
oxidation.

2 Method

2.1 Laboratory SOA generation and collection

195 A schematic description of the experimental procedure used in this study is shown in Figure 1. Laboratory SOA were generated
by gas-phase ozonolysis of β -pinene or limonene in a 7 L quartz flow tube reactor. More detailed information about this reactor

Formatted: Font color: Blue

Formatted: Font color: Blue

Formatted: Font color: Blue

Formatted: Font color: Blue

Formatted: Font color: Blue

Formatted: Font color: Blue

has been described in previous studies (Tong et al., 2016; Tong et al., 2019). Briefly, 1 mL of β -pinene (99%, Sigma Aldrich) or limonene (99%, Sigma Aldrich) were separately kept in 1.5 mL amber glass vials (VWR International GmbH) as SOA precursor sources. ~~AF flows of 1 bar and 0.1 standard liter per minute (slpm) N₂ (99.999%, Westfalen AG) were used as a carrier gas to introduce the evaporated~~ volatile organic compounds (MFC2/VOE). ~~Another 1 slpm N₂ flow was used as a diluting and carrier gas (MFC1) to introduce the gas phase precursors~~ into the reactor for ~~~2.55 min~~ gas-phase ozonolysis reaction. The O₃ was generated via passing synthetic air (Westfalen AG, ~~1.78~2.1 L min⁻¹~~) through ~~MFC3 and~~ a 185 nm UV light (O₃ generator, L.O.T.-Oriol GmbH & Co. KG). The ozone concentrations in the flow tube reactor were 50±10 ppb, 315±20 ppb or 565±20 ppb, which were measured with an ozone monitor (model 49i, Thermo Fisher Scientific Inc.). ~~On the basis of~~Based on a calibration function measured by gas chromatography–mass spectrometry, the precursor concentration was estimated to be in the range of ~~1.2~2.4 ppm~~ for β -pinene and ~~1~3 ppm~~ limonene. ~~The experimental reaction conditions, aerosol concentrations, and collection efficiencies of this study~~ are shown in Table S1. Ozonolysis of β -pinene and limonene SOA were performed under dark and dry conditions to reduce the complexity of SOA formation. Seed aerosols and hydroxyl radical scavenger were not added. When concentrations of β -pinene SOA, limonene SOA, and ozone are stable, the SOA were collected twice in a row for each ozone concentration condition on 47 mm diameter Omnipore Teflon filters (JVWP04700, Merck Chemicals GmbH). The sampling time varied from ~~several~~ minutes to ~~several~~ hours depending on the required aerosol mass. SOA filter samples were wrapped in aluminum foil and kept cool during transport between laboratories. A scanning mobility particle sizer (SMPS, GRIMM Aerosol Technik GmbH & Co. KG) was used to characterize the size distribution, ~~and~~ number concentration, ~~and mass concentration~~ of the generated SOA. A flow rate of ~~~3~2.8 L min⁻¹~~ was controlled using a common diaphragm vacuum pump (0~3 L min⁻¹), which was connected ~~after with~~ the aerosol samplers. ~~Experimental tests confirmed that blank filters did not produce aqueous phase radicals (Tong et al., 2016).~~ The condensation of water vapor on a filter during SOA collection ~~and wall loss~~ were negligible in this study. A Teflon filter with particle loading was weighed using XSE105DU balance with accuracy of ±10 μ g. ~~It is noted that dilution induced an oxygen concentration drop in the flow tube. The impacts of oxygen concentration on HOMs formation and evolution are out of the interest of this study but warranty to be explored in follow up studies.~~

2.2 FT-ICR MS measurement

~~To measure water-soluble organic compounds,~~ the β -pinene and limonene SOA filter samples and blank filters were extracted three times with ultrapure Milli-Q water. Each extraction was carried out in a sonicating ice bath for 10 min. The extracts were combined and added to a solid-phase extraction (SPE) cartridge (Oasis HLB, Waters Corporation, 60 mg, 3 mL) on the Supelco Visiprep SPE Vacuum Manifold (USA), which had been preconditioned with 3×63 mL methanol and Milli-Q water, respectively. Then, the cartridges were washed three times with 6 mL Millipore Q water and dried under a nitrogen flow for around 1 h. Subsequently, the organic compounds retained on the cartridge were eluted using 6 mL of methanol. The eluate was immediately concentrated to about 10 μ L by a rotary evaporator and sample concentrator to ~~optimize/achieve the minimum~~

Formatted: Font color: Blue

Formatted: Font color: Blue

Formatted: Font color: Blue

Formatted: Font color: Blue

Formatted: Subscript

Formatted: Font color: Blue

Formatted: Font color: Blue

Formatted: Font color: Blue

Formatted: Font color: Blue

Formatted: Font color: Blue

Formatted: Font color: Blue

Formatted: Font color: Blue

Formatted: Font color: Blue

Formatted: Font color: Blue

Formatted: Font color: Blue

Formatted: Font color: Blue

detection concentration of SOA extracts for detection. Low molecular weight compounds (< 100 Da) are expected to be excluded in the rinsing and drying steps of extraction, as reported by Bianco et al (Bianco et al., 2018). Finally, the eluate was stored at -20 °C in a brown glass vial with TEFLON® cap until analysis.

The chemical composition of ~~analyte inorganics for~~ pretreated extracts were finally analyzed with a 7 T FT-ICR MS (Bruker Daltonik, GmbH, Bremen, Germany) equipped with an electrospray ionization (ESI) ion source at the School of Earth System Science, Tianjin University, Tianjin, China. The instrument was externally calibrated in the negative ion mode with Suwannee River fulvic acid (SRFC) standard and the resulting mass accuracy was better than 1 ppm. ~~Because the target species were water-soluble polar compounds, all the extract samples were infused into the ESI unit by syringe infusion at a flow rate of 220 μL h⁻¹ and were analyzed in the negative ionization mode and infused into the ESI unit by syringe infusion at a flow rate of 220 μL h⁻¹.~~ Ions were accumulated for 0.05 s in the hexapole collision cell. ~~For each mass spectra were ranged~~ from 150 to 1000 Da. The ESI capillary voltage was 5.0 kV and the spectra are based on the accumulation of 256 scans. An average resolving power (m/Δm 50 %) of over 400 000 (at mass-to-charge (m/z) 400 Da) was achieved. The capillary temperature was maintained at 200 °C. Filter blank was analyzed following the same procedure as the aerosol sample ~~s-analysis~~. Other details of the experiment setup can be found elsewhere (Cao et al., 2016; Xie et al., 2020a).

2.3 Molecular formula assignment

The original FT-ICR MS data was processed using Data Analysis 5.0 (Bruker Daltonics). The mass spectra were internally recalibrated using an abundant homologous series of oxygen-containing organic compounds in the samples over the mass range between 150 and 1000 Da. Molecular formulae were assigned for peaks with a signal-to-noise (S/N) ratio ≥ 4 by allowing a mass error threshold of ±1 ppm between the measured and theoretically calculated mass. The molecular formula calculator was set to calculate formulae in the mass range between 150 and 800 Da with elemental compositions up to 40 carbon (C), 80 hydrogen (H), and 30 oxygen (O) atoms with a tolerance of ±1 ppm when only C, H and O are studied. Furthermore, ~~double bond equivalents (DBE) must be an integer value, the elemental ratio limits of hydrogen-to-carbon ratio (H/C) (0.3~2.5), oxygen-to-carbon ratio (O/C) (0~1.2) and a nitrogen rule for even electron ions were used to eliminate chemically unreasonable formula (Koch et al., 2005). Unambiguous molecular formula assignment was determined with help of the homologous series approach for improving the reliability on multiple formula assignments (Koch et al., 2007). No isotopic peaks were considered in this study, but more information on the FTICR-based analysis of isotopes in ambient aerosols can be found from our previous study- (Xie et al., 2022). To minimize the effects of the experimental procedure, all samples were subtracted from the blank test for organic molecules with the S/N ≥ 20 and intensity greater than those of the analyzed samples were blank corrected.~~ The lower peak intensity of common ions suggests that they were resulted from carry-over within the electrospray ionization source (Kundu et al., 2012). ~~In addition, because of the instrument limitation, the absolute mass concentration of each compound cannot be obtained.~~

The assigned molecular formulae were examined using the DBE and Kendrick mass defect (KMD) series (Wu et al., 2004). To assess the saturation and oxidation degree of β-pinene and limonene SOA, the value of DBE is calculated along Eq. (1).

Formatted: Font color: Blue

Formatted: Font color: Blue

Formatted: Font color: Blue

Formatted: Font color: Blue

Formatted: Font color: Blue

Formatted: Font color: Blue

Formatted: Font color: Blue

Formatted: Font color: Blue

Formatted: Font color: Blue

Formatted: Font color: Blue

Formatted: Font color: Blue

Formatted: Font color: Blue

Formatted: Font color: Blue

Formatted: Font color: Blue

Formatted: Font color: Blue

Formatted: Font color: Blue

$$DBE = 1 + C - 0.5H, \quad (1)$$

where C and H are the number of carbon and hydrogen atoms, respectively.

The maximum carbonyl ratio (MCR) was used to estimate the contribution of carbonyl equivalent groups in the molecule with oxygen number greater than or equal to DBE (Zhang et al., 2021). The value of MCR is calculated as Eq. (2).

$$MCR = \frac{DBE}{O}, \quad (2)$$

where O is the number of oxygen atoms in the formula. Based on the MCR values, the HOMs were categorized into 4 groups: (I) very highly oxidized organic compounds (VHOOCs; $0 \leq MCR \leq 0.2$), (II) highly oxidized organic compounds (HOOCs; $0.2 < MCR \leq 0.5$), (III) intermediately oxidized organic compounds (IOOCs; $0.5 < MCR \leq 0.9$), and (IV) oxidized unsaturated organic compounds (OUOCs; $0.9 < MCR \leq 1$).

The carbon oxidation states (OS_C) is used to describe the composition of complex mixtures of organic matter undergoing oxidation processes. OS_C is calculated as follows (Kroll et al., 2011) (Kroll et al., 2011a):

$$OS_C = 2O/C - H/C, \quad (3)$$

The weighted average of molecular weight (MW), O atom, O/C ratio, OS_C and DBE was calculated using Eq. (4).

$$X = \frac{\sum(Int_i \times X_i)}{\sum Int_i}, \quad (4)$$

where X is the mean value weighted average of different elemental characteristics parameter (above X_i), is the parameter values above and Int_i is the mass spectra peak relative intensity for each individual formula, i .

Molecular corridors can help to constrain chemical and physical properties as well as reaction rates and pathways involved in organic aerosol evolution (Shiraiwa et al., 2014). Saturation vapor pressure (C_0) is a consequence of the molecular characteristics of molar mass, chemical composition, and structure. Li et al. have developed a parameterization to estimate C_0 as $\log_{10}C_0 = f(n_C, n_O)$ (Li et al., 2016). The C_0 is defined by the 2D volatility basis set (2D-VBS) as follows,

$$\log_{10}C_0 = (n_C^0 - n_C)b_C - n_O b_O - 2 \frac{n_C n_O}{n_C - n_O} b_{CO}, \quad (5)$$

where n_C^0 is the reference carbon number; n_C and n_O denote the number of carbon and oxygen atoms, respectively; b_C and b_O denote the contribution of each kind of atoms to $\log_{10}C_0$, respectively, and b_{CO} is the carbon-oxygen nonideality (Donahue et al., 2011). The above parameterization method s obtained at 298 K of this work were as adapted to the work of Li et al. (2016).

The target compounds were grouped categorized into (I) intermediate volatility organic compounds (IVOCs; $300 < C_0 < 3 \times 10^6 \mu\text{g m}^{-3}$), (II) semi-volatility organic compounds (SVOCs; $0.3 < C_0 < 300 \mu\text{g m}^{-3}$), (III) low-volatility organic compounds (LVOCs; $3 \times 10^{-5} < C_0 < 0.3 \mu\text{g m}^{-3}$), (IV) extremely low-volatility organic compounds (ELVOCs; $3 \times 10^{-9} < C_0 < 3 \times 10^{-5} \mu\text{g m}^{-3}$), and (V) ultra-low-volatility organic compounds (ULVOCs; $C_0 < 3 \times 10^{-9} \mu\text{g m}^{-3}$) respectively (Donahue et al., 2011; Bianchi et al., 2019; Schervish and Donahue, 2020).

In order to compare the composition difference between β pinene SOA and limonene SOA, the data of the samples collected twice for the corresponding conditions were integrated and pooled in a subsequent study to investigate the effect of ozone

Formatted: Font color: Blue

Formatted: Font color: Blue

Formatted: Font color: Blue

Formatted: Font color: Blue

Formatted: Font color: Blue

Formatted: Font: Not Italic

Formatted: Font: Not Italic

Formatted: Font: Not Italic

Formatted: Font: Not Italic

Formatted: Font: Not Italic

Formatted: Font: Not Italic

Formatted: Font color: Blue

Formatted: Font color: Blue

Formatted: Font color: Blue

Formatted: Font color: Blue

Formatted: Font: Not Italic

Formatted: Font color: Blue

Formatted: Font: Not Italic

Formatted: Font: Not Italic

Formatted: Font: Not Italic

Formatted: Font color: Blue

concentration on the organic fraction. The relative abundance (RA) is the value of the intensity of the organic molecule divided by the maximum intensity in the corresponding sample.

2.4 Determination of highly oxygenated molecules (HOMs)

Due to their low saturation vapor pressure, ambient HOMs (Vogel et al., 2016) and laboratory-generated HOMs (Jokinen et al., 2015; Roldin et al., 2019; Peräkylä et al., 2020), frequently comprise low-volatility organic compounds (LVOCs) or even extremely low-volatility organic compounds (ELVOCs) (Vogel et al., 2016). In this study, HOMs with molecular formulae of $C_{8-10}H_{12-16}O_{6-9}$ and $C_{17-20}H_{26-32}O_{8-15}$ were used for assigned to HOMing the detected monomers and dimers formed from monoterpene ozonolysis, and compounds with O/C ratio < 0.7 was used to filter out non-HOM monomers (Tu et al., 2016; Tröstl et al., 2016; Tong et al., 2019). The formation pathways of HOMs were estimated based on previous research, and mainly through hydroperoxide channel and Criegee channel (Tomaz et al., 2021; Shen et al., 2021; Kundu et al., 2012). In this paper, monomer refers to C_{8-10} molecule, dimer refers to C_{17-20} molecule. It is noted that the current definition of HOMs does not count in HOM trimmers or other HOMs with higher oligomerization degrees, which is warranty to be explored in follow up studies.

3 Results and discussion

3.1 Effects of ozone concentration on size distribution and oxidation state of SOA

Figure 2 shows the averaged particle size distributions and number concentration of β -pinene SOA and limonene SOA during the aerosol sampling period. Overall, limonene SOA exhibit a broader size distribution range than β -pinene SOA at lower O_3 concentrations (50 and 315 ppb), and the number-size distribution of limonene SOA at 315 ppb O_3 exhibits a shoulder peaks profile, which is different from the mono peak profile of β -pinene SOA. As the ozone concentration is increased from 50 to 565 ppb, the peak number concentration of β -pinene and limonene SOA increased for 5-fold (from 0.7 to $3.5 \times 10^6 \text{ cm}^{-3}$) and 1.8-fold (from 2.2 to $3.9 \times 10^6 \text{ cm}^{-3}$), respectively. Accordingly, the dominant size range of β -pinene and limonene SOA expanded from 10~80 to 10~200 nm and from 10~100 to 10~200 nm, and the size of particles with peak number concentrations shifted from both 32 nm to 70 and 80 nm, respectively are shown in Figure 2, which typically ranged from 20 to 200 nm, and Based on the preassigned particle density of 1 g cm^{-3} , the ~100 nm diameter β -pinene SOA and ~123 nm diameter limonene SOA particles that formed at 565 ppb O_3 exhibit the highest mass concentration of ~1152 and ~1484 $\mu\text{g m}^{-3}$, respectively (Figure S1 in SI) median diameters of the mass size distribution were 35~80 nm. The precursor-dependent number- and mass-size distribution profiles in Figures 42 and S1 may be related to different partition and agglomeration kinetics of low volatile organics, with the former process playing a plausible stronger role. The "partition" here means an equilibrium between the absorption and desorption rates of oxidized β -pinene or limonene products from SOA surfaces (Kamens et al., 1999), and a gas/particle partitioning absorption model has been found able to describe SOA yield well

Formatted: Font color: Blue

Formatted: Font color: Blue

Formatted: Font color: Blue

Formatted: Font color: Blue

Formatted: Font color: Blue

Formatted: Font color: Blue

Formatted: Font color: Blue

Formatted: Font color: Blue

Formatted: Font color: Blue

Formatted: Font color: Blue

Formatted: Font color: Blue

Formatted: Font color: Blue

Formatted: Font color: Blue

Formatted: Font color: Blue

Formatted: Not Superscript/ Subscript

Formatted: Not Superscript/ Subscript

Formatted: Font color: Blue

Formatted: Font color: Blue

Formatted: Font color: Blue, Superscript

Formatted: Font color: Blue

Formatted: Font color: Blue

Formatted: Font color: Blue

Formatted: Font color: Blue

Formatted: Font color: Blue

Formatted: Font color: Blue

Formatted: Font color: Blue

Formatted: Font color: Blue

Formatted: Font color: Blue, Superscript

Formatted: Font color: Blue

Formatted: Font color: Blue

Formatted: Font color: Blue

(Takekawa et al., 2003; Song et al., 2011). The higher SOA yield and number concentration of β -pinene SOA and limonene SOA at higher ozone concentrations, which may be due to the formation of high molecular weight and low volatile dimers (Kristensen et al., 2014). It is associated with the accelerated condensation or gas-particle partition of low-volatile organics at higher ozone concentrations, which can promote the formation and growth of molecular clusters and survive to cloud condensation nuclei active sizes (Shrivastava et al., 2017). This claim is supported by previous findings that ozonolysis of limonene and monoterpenes exhibits high yield of extremely-low volatile organic compounds (ELVOCs) and can produce substantial amounts of SOA even at low ozone concentrations (Waring et al., 2011) (Waring et al., 2011; Jokinen et al., 2015). Waring et al. (2011) found that limonene produced higher initial nucleation in low ozone experiments. This may also be the reason why at ozone concentrations of 50 ppb the particle size of limonene SOA exhibit a broader distribution than β -pinene SOA at ozone concentrations of 50 ppb, indicating a plausible different partition and agglomeration kinetics of them. In addition, β -pinene SOA and limonene SOA may differ in terms of gas-particle partition. Partition can be expressed as a balance between the rate of oxidized precursor products absorption and the rate of precursor products loss from the aerosol system (Kamens et al., 1999). Limonene is more oxidized than β -pinene and may increase the particle size range by forming highly oxidized organics that are partitioned into the particle phase.

The molecular weight (weighted average of MW), O atom number, O/C ratio, double bond equivalents (DBE), and carbon oxidation state (OS_C), and VOC subgroups of β -pinene SOA and limonene SOA OS_C increased with the increase of ozone concentration were shown in for β -pinene SOA (Table 1). It shows that particulate organics with higher oxidation OS_C and higher carbon number-MW, and lower volatility organic matter exhibit larger contribution to SOA mass prefer to form at higher ozone concentration, and most of the less oxidized organic molecules may be converted into highly oxidized organic molecules (HOMs). Results also show that high concentration of ozone tends to convert less oxidized organic molecules to highly oxygenated organic molecules (HOMs) via increase oxygen reaction producing oxygen-increasing reactions on the carbon skeleton. This means that in the oxygen-increasing reactions, i.e., addition of one more oxygen atom to the intermediate alkoxy radicals resulting from the precursors ozonolysis converts to form a new alkoxy radicals (Kundu et al., 2012). The overall higher fraction of ULVOCs in β -pinene SOA than limonene SOA is in line with previously observed higher abundance of organic peroxides and aqueous radical yield of β -pinene SOA (Badali et al., 2015; Tong et al., 2016; Tong et al., 2018). This may indicate reflects the importance of ozone concentration in the formation of particulate organic peroxides by determining redox activity of SOA ozonation of β -pinene. For limonene SOA, when the ozone concentration was increased from 315 to 565 ppb, the MW, O atom and DBE are decreased, indicating that high carbon- and oxygen-containing organic molecules in limonene SOA may fragment at high ozone concentration to form low carbon number and less oxidized organic molecules. The element characteristic values of limonene SOA were generally higher than β -pinene SOA, probably due to the following reasons. First, ozonolysis of limonene proceeds in a faster rate ($k_{\text{limonene}+\text{O}_3} = 2.1 \times 10^{-16} \text{ cm}^3 \text{ molecules}^{-1} \text{ s}^{-1}$) than β -pinene ($k_{\beta\text{-pinene}+\text{O}_3} = 1.5 \times 10^{-17} \text{ cm}^3 \text{ molecules}^{-1} \text{ s}^{-1}$) (Atkinson and Arey, 2003). Second, limonene is more inclined to

Formatted: Font color: Blue

Formatted: Font color: Blue

Formatted: Font color: Blue

Formatted: Font color: Blue

Formatted: Font color: Blue

Formatted: Font color: Blue

Formatted: Font color: Blue

Formatted: Font color: Blue

Formatted: Font color: Blue

Formatted: Font color: Blue

Formatted: Font color: Blue

Formatted: Font color: Blue

355 undergo oxygenate and accretion reactions than β -pinene. Third, non-condensation reactions might play a more important role in the limonene SOA formation (Kundu et al., 2012).

360 The higher abundance of organic peroxides in β -pinene SOA than limonene SOA can explain the higher yield of $\cdot\text{OH}$ of β -pinene SOA in liquid water (Tong et al., 2016). Figure S1a-S2a shows that the summed total MS spectra intensity of identified the organic signal in the β -pinene SOA and limonene SOA samples, and the compounds with MW of 150-450 Da account for a major fraction. As the ozone concentration was increased from 50 to 315 and 565 ppb, the total spectra intensity of β -pinene SOA increased significantly continuously with the increase of ozone concentration, whereas that of limonene increased first and then decreased. Figure S12b shows, while the formula number concentration of assignable organic molecules in SOA, s. The total formula number of β -pinene SOA increased first and then decreased as the increasing ozone concentrations reached the maximum value at 315 ppb ozone concentration. In contrast, the total intensity of the organic signal in the limonene SOA sample reached the maximum value at 315 ppb ozone concentration, but and the formula number of of limonene SOA gradually decreased. organic molecules decreased significantly with the increase of ozone concentration. The peak intensity of MW ranged from 350 to 450 Da, with β -pinene SOA exhibit a maximum proportion at 565 ppb ozone, but limonene SOA have the highest proportion at 315 ppb. The different trends from summed MS spectra intensity to formula number reflect the is complexity of SOA mass and composition evolution, which varied as precursor type trend indicates that MW of biogenic SOA formed from different precursors have different responses to ozonolysis.

370 Table S2 shows that for β -pinene SOA, the predominant molecules in β -pinene SOA are $\text{C}_{17}\text{H}_{26}\text{O}_4$ ($m/z = 274-293(\text{C}_{17}\text{H}_{26}\text{O}_4)$) and $\text{C}_{10}\text{H}_{16}\text{O}_3$ ($m/z = 183-183(\text{C}_{10}\text{H}_{16}\text{O}_3$, pinonic acid) at 50 ppb ozone concentration (Jaoui and Kamens, 2003) at 50 ppb ozone concentration, and $\text{C}_{19}\text{H}_{30}\text{O}_5$ ($m/z = 337(\text{C}_{19}\text{H}_{30}\text{O}_5)$, $\text{C}_{10}\text{H}_{16}\text{O}_3$ ($m/z = 183(\text{C}_{10}\text{H}_{16}\text{O}_3$, $\text{C}_9\text{H}_{14}\text{O}_4$ ($m/z = 186-185(\text{C}_9\text{H}_{14}\text{O}_4)$, and $\text{C}_{19}\text{H}_{30}\text{O}_7$ ($m/z = 370-369(\text{C}_{19}\text{H}_{30}\text{O}_7)$) at 315 ppb and 565 ppb ozone concentrations. A higher abundance relative abundance (RA) of $\text{C}_{32}\text{H}_{42}\text{O}_3$ ($m/z = 474-473(\text{C}_{32}\text{H}_{42}\text{O}_3)$) molecule was only found in β -pinene SOA formed at 50 ppb ozone condition, which is high carbon-containing and less oxygen-containing compound, indicating that β -pinene ozonolysis products prefer carbon-carbon bonding or oligomerizing at low ozone concentration. The mostly abundant organics in limonene SOA is always 7-hydroxy limononic acid ($\text{C}_{10}\text{H}_{16}\text{O}_4$, the molecule of $m/z = 199(\text{C}_{10}\text{H}_{16}\text{O}_4$, 7-hydroxy limononic acid) at in three ozone concentrations, which has also been observed as a major product from limonene oxidation by ozone ozonolysis in previous studies (Kundu et al., 2012; Gallimore et al., 2017; Hammes et al., 2019). Low oxygen-containing organic molecules (monomer: $\text{O} \leq 2$ and dimer: $\text{O} \leq 4$) exhibit a higher relative abundance in β -pinene and limonene SOA. At at 50 ppb lower ozone concentration, both β -pinene SOA and limonene SOA exhibited higher abundance RA of organic molecules with less oxygen-containing (monomer: $\text{O} \leq 2$ and dimer: $\text{O} \leq 4$), while the abundance RA of organic molecules with less oxygen-containing was quite low at 565 ppb ozone condition. This indicates that high ozone concentration is not conducive to the formation of less oxygen-containing organic molecules their faster or promotes the conversion of less oxidized organic molecules into high oxygen-containing organic molecules via accelerated autooxidation by higher concentrations of ozone.

Formatted: Font color: Blue

Formatted: Font color: Blue

Formatted: Font color: Blue

Formatted: Font color: Blue

Formatted: Font color: Blue

Formatted: Font color: Blue

Formatted: Font color: Blue

Formatted: Font color: Blue

Formatted: Font color: Blue

Formatted: Font color: Text 1

Formatted: Font color: Blue

Formatted: Font color: Blue

Formatted: Font color: Blue

Formatted: Font color: Blue

Formatted: Font color: Blue

Formatted: Font color: Blue

Formatted: Font color: Blue

390 For a better characterization of the formation and evolution processes of SOA, ~~For limonene SOA, when the ozone~~
~~concentration is increased from 315 ppb to 565 ppb, the MW, O-atom and DBE are decreased, indicating that the high carbon-~~
~~containing and oxygen-containing organic molecules in limonene SOA may crack fragment at high ozone concentration to~~
~~form low carbon number and less oxidized organic molecules. The element characteristic values of SOA produced by limonene~~
~~were generally higher than those of β -pinene, probably due to the faster rate at which ozonolysis proceeds for limonene~~
~~($k_{\text{limonene}+\text{O}_3} = 2.1 \times 10^{-16} \text{ cm}^3 \text{ molecules}^{-1} \text{ s}^{-1}$) as compared to β -pinene ($k_{\beta\text{-pinene}+\text{O}_3} = 1.5 \times 10^{-17} \text{ cm}^3 \text{ molecules}^{-1} \text{ s}^{-1}$) (Atkinson~~
~~and Arey, 2003). This shows that limonene is preferred to proceed oxygenate and aceretion reactions than β -pinene. Compared~~
~~to the precursor β -pinene, the unique SOA formed by ozonation of limonene is more concentrated in high OS_c and O/C ratio,~~
395 as well as low H/C ratio organic molecules. It seems that the non-condensation reaction channel (Kundu et al., 2012) of
limonene is more important than β -pinene. Perhaps the high oxygen-containing organic matter contributes more to the larger
size particles of molecular clusters.

The maximum carbonyl ratio (MCR) index ~~was used here~~ ~~is suggested as a tool for a better characterization of the sources and~~
~~the processing of atmospheric OA components (Zhang et al., 2021). Figure 3 shows the components of β -pinene SOA and~~
400 limonene SOA ~~contained HOMs~~ depicted in an MCR-Van Krevelen (VK) diagram. ~~The largest fraction~~ ~~Most of β -pinene~~
~~SOA components~~ ~~the plotted compounds at 565 ppb ozone concentration (66%) and the largest fraction of limonene SOA~~
~~components at 315 ppb ozone concentration (59%) are located in regions II and III, with the former region covers more~~
~~compounds, while~~ ~~Only a few compounds show up in regions I and IV. Such a distribution pattern indicates that most of the~~
405 ~~aerosolized HOMs oxidation products formed from ozonolysis~~ ~~oxidation of β -pinene and limonene are intermediately~~
~~oxidized organic compounds (IOOCs) and oxidized unsaturated organic compounds (OUOCs)~~ ~~moderately oxidized, with MCR~~
~~values of 0.52 ~ 1.00.5. Very little amount of and only a few of them organic compounds with have MCR values between~~
~~0 ~ 0.2 or > 0.9, reflecting the low abundance of highly oxidized organic compounds (HOOCs) or highly unsaturated organic~~
~~compounds (HUOCs). It is noted that MRC cannot differentiate the functional groups with the same formular, the improvement~~
~~of which is warranty to be explored in follow up studies. The organic compounds with higher relative abundance (RA) fall~~
410 ~~mainly in the region III. Interestingly, the maximum relative larger RA value abundance value of HOMs in β -pinene SOA~~
~~increased~~ ~~delevated as the increasing ozone concentration, whereas the that of larger RA value HOMs in limonene SOA~~
~~decreased~~ ~~accordingly with increasing ozone concentration. Thus, It seems that high the 565 ppb concentration of ozone might~~
~~concentration have some inhibitory effect on the oxidation of limonene to form formation of limonene SOA-associated~~
~~organic compounds HOMs (e.g., due to ozonolysis produced OH radicals begin to cause more oxidative fragmentation at high~~
415 ~~O₃ levels), whereas an enhancement effect on the formation of β -pinene SOA-associated organic compounds.~~

3.2 Composition and relative abundance of HOMs in β -pinene and limonene SOA

As shown in Figure 4, the identified HOMs mainly exist ~~as dimers~~ with m/z of 350~450 Da. ~~Therein, the relative fractions of~~
420 ~~HOMs (RA_{HOMs}) in limonene SOA has higher RA_{HOMs} are higher than β -pinene SOA. As the ozone concentration was~~

Formatted: Font color: Blue

Formatted: Font color: Blue

Formatted: Font color: Blue

Formatted: Font color: Blue

Formatted: Font color: Blue

Formatted: Font color: Blue

Formatted: Not Superscript/ Subscript

Formatted: Font color: Blue, Superscript

Formatted: Font color: Blue

Formatted: Font color: Blue

Formatted: Font color: Blue

Formatted: Font color: Blue, Subscript

Formatted: Font color: Blue

Formatted: Font color: Blue

Formatted: Font color: Blue

increased from 50 to 315 ppb, the MS spectra peak number-based RA_{HOMs} in β -pinene and limonene SOA kept constant to be ~3% and ~5%, whereas the peak intensity-based RA_{HOMs} increased significantly from 3% to 7% and 14% to 20%, respectively. This indicates that HOMs yield rather than chemical composition diversity of β -pinene and limonene SOA responded to the increasing oxidation degree of precursors or ozone concentration. As the ozone concentration is/was increased further to 565 ppb, both of the peak number- and peak intensity-based RA_{HOMs} in β -pinene SOA increased significantly to 135% and 513%, respectively, indicating a prominent change of HOMs yield and composition. In contrast, and the peak number-based RA_{HOMs} in limonene SOA still did not change, and the peak intensity-based RA_{HOMs} even decreased slightly to 18%, reflecting the main change of HOMs yield. It has been previous studies foundly reported that in limonene ozonolysis experiments, the addition of O_3 occurs mainly on the endocyclic double bond, which and the endocyclic double bond tends to generate 'OH via the hydroperoxide channel, and, while a higher proportion of stabilized Criegee intermediates (SCIs) can be formed from the exocyclic double bond than from the endocyclic double bond (Wang and Wang, 2021; Gong et al., 2018). Thus/Therefore, we estimate that, under high ozone concentration conditions, the ozonolysis of β -pinene produced more HOMs, whereas the overoxidation and disassociation of preformed particulate HOMs may happen to limonene SOA the more 'OH produced by the ozonation of endocyclic double bond of limonene may compete with O_3 and affect towards the formation and evolution of particulate HOM dimers (Atkinson et al., 1992; Kristensen et al., 2016).

Figure 5 shows the O/C, H/C, carbon number, and OS_C of common or unique HOMs and non-HOM molecules in β -pinene SOA, and limonene SOA, or and HOMs formed under three ozone concentrations samples. Green data points were found more than red data points, meaning that The comparison revealed that the larger number of molecules formed by ozonolysis of β -pinene was higher than by limonene. The oxidation state distribution of oxidation states in the unique molecules (i.e., compounds that were only found) of in β -pinene SOA was broad (Figure 5a) and mostly are located in the low O/C ratio region of lower O/C ratio ~0.4 (Figure 5b). In contrast, while most of the unique molecules in limonene SOA were distributed in higher are located in the high oxidation state region of $OS_C > -1.5$ and lower H/C ratio (Figure 5a and 5b) and moderate O/C ratio region of 0.3~0.7 (Figure 5b). Such a profile difference, indicating indicates a higher ozonation degree of limonene than that of β -pinene. The HOMs (in Figure 5c and 5d) showed a similar variation trends as the SOA (Figure 5a and 5b), confirming the close association/contribution of HOMs with to the formation of biogenic SOA. The substantial number of grey data points in Figure 5a-5d reflects the significant composition similarities between β -pinene and limonene SOA, including the HOMs.

The identified identified HOMs in β -pinene and limonene SOA are categorized into groups with different carbon number (C_n) or oligomer clusters, and their relative fractions RA_n of which are plotted versus the ozone concentration in Figure 6. Figure 6a shows that HOM monomers are mostly enriched in the respective distribution pattern of HOM monomers in β -pinene and limonene SOA that formed at 315 ppb ozone condition kept the same under different ozone concentrations. Therein, the the HOM monomers in limonene SOA contained HOM monomers are mainly exist as C_{10} species, while HOM monomers in β -pinene SOA contained HOM monomers mainly comprise compounds with eight carbon atoms (exist as C_8 species). This may be isis due to the fact that the carbon backbone of

Formatted: Font color: Blue

Formatted: Font color: Blue

Formatted: Font color: Blue

Formatted: Font color: Blue

Formatted: Font color: Blue

Formatted: Font color: Blue

Formatted: Font color: Blue

Formatted: Font color: Blue

Formatted: Font color: Blue

Formatted: Font color: Blue

Formatted: Font color: Blue

Formatted: Font color: Blue

Formatted: Font color: Blue

Formatted: Font color: Blue

Formatted: Font color: Blue

Formatted: Font color: Blue

Formatted: Font color: Blue

Formatted: Font color: Blue

Formatted: Font color: Blue

455 endocyclic limonene is retained on ozonolysis, whereas the terminal vinylic carbon of exocyclic β -pinene is cleaved (Ma and Marston, 2008; Kundu et al., 2012). Figure 6b shows that the ~~relative abundance RA_{HOMs} of dimmers dimers~~ in β -pinene and limonene SOA exhibits different variation trends as the increasing of ozone concentrations. ~~About the β -pinene SOA, T~~ the carbon numbers of HOM ~~dimmers dimers in β -pinene SOA exhibit~~ have the same pattern at 50 and 315 ppb ozone concentrations, with the ~~relative abundance~~ RA increased from C_{17} to C_{18} and then gradually decreased for C_{19} and C_{20} species. However, at 565 ppb ozone condition, the ~~RA relative abundance~~ of HOM dimers continually decreased from C_{17} to C_{20} compounds. In contrast, the C_n pattern of HOM dimers in limonene SOA kept the same under different ozone concentrations, which reached a maximum for C_{19} species. The different C_n patterns of HOM dimers in β -pinene and limonene SOA may be due to the ~~front former~~ ones tend to form via the combination of C_8 and C_9 , or C_9 and C_9 , whereas the later ones are preferred to form via the combination of C_{10} and C_9 . Such an ~~inference explanation may also explain~~ agrees with the higher averaged carbon number, oxygen number, and molecule weight of limonene SOA than β -pinene SOA (Table 1).

3.3 Volatility of HOMs in β -pinene and limonene SOA

465 ~~To explore the volatility of HOMs in β -pinene and limonene SOA, the were categorized in identified HOMs haven been assigned to semi-, low-, and extremely low-volatile organic compounds (SVOCs, LVOCs, and ELVOCs) for exploring their volatility distribution and their RA were shown in Figure 7.~~ Figure 7a shows that ~~the HOMs in both β -pinene and limonene SOA mainly exist as LVOCs subgroup dominants the peak intensity of both β -pinene and limonene SOA contained HOMs, but their MS spectra intensity-based relative abundances (RA_{HOMs}) pattern of which at three ozone concentrations exhibit different patterns, i.e., increased as increasing ozone concentration for β -pinene SOA, while reached the maximum value at the ozone concentration of 315 ppb for limonene SOA. Moreover, the RA_{HOMs} pattern of LVOCs resembles the combined RA_{sum} of SVOCs, LVOCs, and ELVOCs, reflecting the strong impact of low volatile species on SOA's volatility and oxidation state. Moreover, the RA of LVOC type HOMs in β -pinene SOA increases with increasing ozone concentration, while that in limonene SOA reaches the maximum value at the ozone concentration of 315 ppb.~~ Figure 7b shows that formula number-based total ~~RA_{HOMs} RA~~ of SVOCs, LVOCs, and ELVOCs increased as the increasing of ozone concentrations for both β -pinene and limonene SOA, with the ~~RA relative abundance~~ of LVOCs equivalent to the ELVOCs. Thus, Figure 7 reflects that mass variation of β -pinene and limonene SOA during ozone chemistry are largely driven by LVOCs and ELVOCs. ~~In addition~~ Moreover, the peak intensity- and formula number-based RA_{HOMs} of LVOCs and ELVOCs in limonene SOA is significantly higher than that of β -pinene SOA, indicating a higher contribution of that LVOCs and ELVOCs contribute more to the HOMs in limonene SOA. These findings agree with previous discovery of limonene ozonolysis ~~as to be~~ more efficient ELVOCs formation pathway than β -pinene ozonolysis in generating ELVOCs (Jokinen et al., 2015) (Jokinen et al., 2015a). Moreover, ~~the~~ The volatility and carbon oxidation state averages of HOMs were also found to change in similar trends as that of LVOCs, ELVOCs, and ULVOCs in SOA, but the trends of β -pinene SOA and limonene SOA are different (as shown in Figure S2S3).

Formatted: Font color: Blue

Formatted: Font color: Blue

Formatted: Font color: Blue

Formatted: Font color: Blue

Formatted: Font color: Blue

Formatted: Font color: Blue

Formatted: Font color: Blue

Formatted: Font color: Blue

Formatted: Font color: Blue

Formatted: Font color: Blue

Formatted: Font color: Blue

Formatted: Font color: Blue

Formatted: Font color: Blue, Subscript

Formatted: Font color: Blue

Formatted: Font color: Blue

Formatted: Font color: Blue

Formatted: Font color: Blue

Figure 8 shows the O/C ratio of β -pinene and limonene SOA constituents versus their estimated volatility. Figure 8a-8c shows that the O/C ratio distribution of ULVOCs in β -pinene SOA is broadened as the increase of ozone concentration. Meanwhile, both of O/C ratios and relative abundance of IVOCs, SVOCs, LVOCs, and ELVOCs increased prominently, whereas the relative abundance of compounds with low O/C ratios decreased. This indicates that deeper oxidation of β -pinene may decrease the overall volatility of SOA particles via changing the relative abundance of organic matter with different volatilities. Figure 8d-8f shows that O/C ratio and volatility distribution of limonene SOA components vary slightly. This may be correlated with the preference of limonene to forming highly oxygenated and low-volatility reaction products by limonene via an autoxidation mechanism (Jokinen et al., 2015). Moreover, the enrichment of high-RA ELVOCs in limonene SOA confirms that limonene is more likely-prone to form particulate ELVOCs even ULVOCs than β -pinene via ozonolysis, which may be related to the higher reactivity of limonene due to its intrinsic two double bonds and endocyclic structure.

Figure 9 shows the molecular corridor of β -pinene and limonene SOA, which is a two-dimensional framework of volatility and molecular weight of SOA components bounded by two boundary lines of n-alkanes (C_nH_{2n+2}) with O/C = 0 and sugar alcohols ($C_nH_{2n+2}O_n$) with O/C = 1, which helps to explaining the physicochemical properties in the evolution of SOA organic aerosols by plotting their component's volatility and molecular weight (Li et al., 2016; Xie et al., 2020b). At 50 ppb ozone concentration, Figure 9 shows the correlation between the volatility and molecular weight of the common and unique molecules of β -pinene SOA and limonene SOA under three ozone conditions. The number of unique organic molecules formed by monoterpene oxidation is higher at 50 ppb ozone concentration, accounting for about 15–20% of the total number of molecules. Furthermore, substantial amounts of unique organic molecules that at 50 ppb ozone concentration are mainly composed of concentrated in the SVOCs and LVOCs regions were observed, the number of which accounts for 15–20% of all the identified molecules for β -pinene or limonene SOA. Smaller amounts of unique organic molecules that mainly composed of ELVOCs and ULVOCs were observed at 315 ppb and 565 ppb ozone concentrations, are mainly concentrated in the ELVOCs and ULVOCs region. This trend suggests the ozonolysis-enhanced formation of low volatile organic species for biogenic precursors. At all three different ozone concentration conditions. Compared to limonene SOA, many more β -pinene SOA always contained more low volatile organic compounds (LVOCs, ELVOCs, and ULVOCs) than limonene SOA, which distributed close to near the sugar alcohol ($C_nH_{2n+2}O_n$) line in Figure 9 (blue dashed line), were found in β -pinene SOA, indicating a greater impact of ozonolysis on β -pinene SOA's volatility diversity. Under 565 ppb ozone condition, indicating that ozone concentration has a greater impact on the SOA formed from ozonolysis of β -pinene. β -pinene SOA comprise substantial fraction of ULVOCs with molar mass of 500–800 g mol⁻¹ account for a substantial fraction of β -pinene SOA formed at 565 ppb ozone. However, limonene SOA were mainly composed of whereas the SVOCs, LVOCs, and ELVOCs with molar mass of 200–600 g mol⁻¹ dominate the limonene SOA. Such a compositional difference The volatility difference of β -pinene and limonene SOA may be associateds with the plausible different partition or stabilization-evolution mechanisms of HOMs and low volatility species under different ozone concentrations, including the SOA aging related volatilization.

Formatted: Font color: Blue

Formatted: Font color: Blue

Formatted: Font color: Blue

Formatted: Font color: Blue

Formatted: Font color: Blue

Formatted: Font color: Blue

Formatted: Font color: Blue

Formatted: Font color: Blue

Formatted: Font color: Blue, Not Highlight

Formatted: Font color: Blue

Formatted: Font color: Blue, Not Highlight

Formatted: Font color: Blue, Not Highlight

Formatted: Font color: Blue

Formatted: Font color: Blue, Not Highlight

Formatted: Font color: Blue

Formatted: Font color: Blue, Not Highlight

Formatted: Font color: Blue, Not Highlight

Formatted: Font color: Blue

Formatted: Font color: Blue, Not Highlight

Formatted: Font color: Blue

Formatted: Font color: Blue

Formatted: Font color: Blue

Formatted: Font color: Blue, Not Highlight

3.4 Potential formation mechanisms of HOM monomers and dimers in β -pinene and limonene SOA

Previous studies show that gas-phase monomer and dimer products formed through radical chemistry of organic peroxides (e.g., $\text{RO}_2 + \text{RO}_2$, $\text{RO}_2 + \text{HO}_2$, RO_2 isomerization, or $\text{RO}_2 + \text{NO}$), reaction of RO_2 with monoterpenes, and reaction of stabilized Criegee intermediate with carboxylic acid can produce gas-phase monomers or dimers, the low volatile fractions of which are expected to form clusters and accommodate onto particles, contributing to SOA formation (Ehn et al., 2014; Clafin et al., 2018; Shi et al., 2022) (Ehn et al., 2014; Clafin et al., 2018) (Ehn et al., 2014; Clafin et al., 2018). But aldehydes and ketones are often converted to carboxyl and ester groups by Baeyer-Villiger reactions with the hydroperoxides and peroxyacid in particle phase, while hydroperoxides and peroxyacid are converted to acids, alcohols, or ketones (Clafin et al., 2018). Furthermore, the reaction of hydroperoxides in organic peroxides also react with aldehydes to produce peroxyhemiacetals, a process in which the vapour pressure decreases and affects the gas-particle partition coefficient (Li et al., 2016a). Due to the high activity of these pathways, the dimers with very low volatility are expected to form clusters and be distributed directly onto particles after gas-phase production. The dimers are strongly influenced by particle-phase chemistry, possibly involving the combined effects of accretion reactions ($\text{C}_{8-10} + \text{C}_{8-10} \rightarrow \text{C}_{17-20}$) and decomposition of high-molecular-weight compounds ($\text{C}_{20} \rightarrow \text{C}_{17-10}$) (Pospisilova et al., 2020). The formation of HOMs dimers is mainly through the accretion reaction of various HOMs monomers RO_2 and the termination reaction of dimer RO_2 formed by the further reaction of the closed-shell dimer with O_3 , and they may also be through C_{10} reaction of RO_2 with monoterpenes (Shi et al., 2022). The HOMs trimers may be formed via the accretion reaction of dimer RO_2 and monomer RO_2 , which will not be analyzed in detail later.

HOMs monomers may be formed via hydroperoxide channel and oxygen-increasing reactions (OIR) of Criegee alkoxy channel (Tomaz et al., 2021; Shen et al., 2021; Kundu et al., 2012). The possible proposed formation mechanisms of C_{10} HOMs monomers during from the ozonolysis of β -pinene and limonene ozonolysis are shown in Figure 10. Therein the hydroperoxide and alkoxy chemistry might have played an important role (Tomaz et al., 2021; Shen et al., 2021; Kundu et al., 2012). There is also the high probability of that ozone first reacts with endocyclic double bond of limonene, which opens the chain to form Criegee alkoxy radical, and then formed $\text{C}_{10}\text{H}_{14}\text{O}_7$, Figure 11 and $\text{C}_{10}\text{H}_{14}\text{O}_8$. Ozone concentration had a great influence on HOMs of C_9 and C_{10} in β -pinene system, and the formation path is as depicted in Figure S3. Here, a number of series of CH_2 homologous series of HOM monomers with CH_2 were found (Fig. 11). Among them for β -pinene SOA, $\text{C}_9\text{H}_{14}\text{O}_7$ and $\text{C}_{10}\text{H}_{16}\text{O}_7$ were found in all three ozone concentrations, but whereas $\text{C}_9\text{H}_{14}\text{O}_8$ and $\text{C}_{10}\text{H}_{14}\text{O}_7$ and $\text{C}_9\text{H}_{12}\text{O}_7$ were only found at 315 ppb and 565 ppb ozone concentrations, and $\text{C}_9\text{H}_{12}\text{O}_8$ was formed at high ozone concentrations. For limonene SOA, $\text{C}_{10}\text{H}_{16}\text{O}_8$ and $\text{C}_{10}\text{H}_{14}\text{O}_7$ were found at all three ozone concentrations. Like previous studies (Ehn et al., 2014; Berndt et al., 2016; Brean et al., 2019), a common monoterpene oxidation product This suggests that β -pinene increases the possibility of carbonyl formation at high ozone concentrations. The formation of $\text{C}_{10}\text{H}_{16}\text{O}_9$ has also been observed in β -pinene SOA in this study or corresponds to the monoterpene oxidation product (Ehn et al., 2014; Berndt et al., 2016; Brean et al., 2019). At high ozone concentrations, in this experiment, only the O numbers of HOM dimers in β -pinene SOA were detected at

Formatted: Font color: Blue

Formatted: Font color: Blue

Formatted: Font color: Blue

Formatted: Font color: Blue

Formatted: Font color: Blue

Formatted: Font color: Blue

Formatted: Subscript

Formatted: Font color: Blue

Formatted: Font color: Blue

Formatted: Font color: Blue

Formatted: Font color: Blue

550 high-ozone concentration, and the O-number of HOMs dimers under this condition could be up to 15, while that for C₁₀H₁₆O₈ was not detected in the limonene SOA, and the maximum O-number of the HOMs dimers was only 13. This may be due to the fact that because the oxidation degree of RO₂ termination reaction of some HOMs in β-pinene SOA is higher than that of in limonene SOA.

The accretion reaction RO₂ + R'O₂ → ROOR' + O₂ formed by the self-self-combination and cross-reaction of RO₂ radicals has been proposed to be generally effective (Berndt et al., 2018b; Bianchi et al., 2019; Kahnt et al., 2018; Ehn et al., 2014; Berndt et al., 2018a). The presence of C₁₇H₂₆O₈ through the decomposition of C₁₉H₂₈O₁₁ with loss of a ketene from the internal containing a labile trioxide functionality, and the conversion of the unstable acyl hydroperoxide groups to carboxyl groups (Kahnt et al., 2018). Tomaz et al. (2021) found that the reaction between C₁₀H₁₅O₆ and C₁₀H₁₅O₈ radicals may also contribute to the formation of C₂₀H₃₀O₁₂ dimer (Tomaz et al., 2021), corresponding monomers and dimers were found in the limonene system, β-pinene at high ozone concentration, C₁₀H₁₆O₈ organic matter, and subsequently detected the C₂₀H₃₀O₁₂ dimer, which verified this conclusion. Alternatively, a weakly bound RO...O₂...R'O cage formed by the asymmetric cleavage of the tetroxide, which then loses O₂, intersystem crosses and alkoxy recombines, also converts to ROOR' (Lee et al., 2016). The combination of an acylperoxy radical (RC(O)O₂) associated with cis-pinic and a RO₂ related to 7- or 5-hydroxypinonic acid allows for a RO₂ + R'O → RO₃R' radical termination reaction, which is also an important pathway for the formation of HOM dimers (Kahnt et al., 2018). C₁₇H₂₆O₈ may be produced by the decomposition of C₁₉H₂₈O₁₁ with a loss of a ketene from the internally containing a labile trioxide function groupality, and the conversion of the unstable acyl hydroperoxide groups to carboxyl groups (Kahnt et al., 2018). According to recent findings, the main pathway for the formation of the accretion product ROOR' is the RO₂ + α-pinene reaction, rather than the RO₂ + R'O₂ reaction (Shi et al., 2022). The alkyl radicals produced by the RO₂ + α-pinene former reaction can also produce HOM dimers and trimers through an autoxidation chain. Even if the RO₂ radical is a RC(O)O₂, it is still prone more likely to react with α-pinene. The chemical formulas along together with

560 suggested molecular structures of the identified dimer compounds are shown in Tables S3. Most of the HOMs products in of β-pinene and limonene SOA the two monoterpenes were very similar, while the RA relative abundance of the different HOMs varied widely, suggesting that the reaction pathways are similar, but the degree of branching in the reaction mechanism is different. Moreover, the rate of dimer formation by self and cross-reacting RO₂ radicals not only depends on the structure of RO₂ radical, but also increases with the size of the RO₂ radical (Berndt et al., 2018a).

575 Accretion reactions transform the mass from monomers to oligomers, yielding products with a higher number of carbon atoms and converting semi-volatile molecules into higher-molecular weight compounds that have with lower saturation vapor concentrations (Barsanti et al., 2017). Accretion reactions are probably exist going on both in both the gas phase and the particle phase, meanwhile some with partial of the gas phase accretion products partition into may be decomposed in the particle phase and undergo further aging process. So Thus, the measured particle-phase dimers may be quite different from the original gas-phase ones (Zhang et al., 2017). These The gas-phase accretion reactions have been studied under laboratory conditions and were also suggested to play an important role in ambient environment (Berndt et al., 2018a). This observation shows that

Formatted: Font color: Blue

Formatted: Font color: Blue

Formatted: Font color: Blue

Formatted: Font color: Blue

Formatted: Font color: Blue

Formatted: Font color: Blue

Formatted: Font color: Blue

Formatted: Font color: Blue

Formatted: Font color: Blue

Formatted: Font color: Blue

Formatted: Font color: Blue

Formatted: Font color: Blue

Formatted: Font color: Blue

Formatted: Font color: Blue

Formatted: Font color: Blue

Formatted: Font color: Blue

Formatted: Font color: Blue

Formatted: Font color: Blue

Formatted: Font color: Blue

585 ~~the particle phase chemistry~~ For this study, we suggest that ~~gas-phase reactions~~ significantly affected ~~causes changes in~~ the overall SOA composition ~~especially the HOMs over at the different~~ ozone concentrations ~~observed here~~. High molecular weight and low volatile dimer ~~compounds~~ have been identified as important components of environmental ~~compounds aerosols~~. The monomeric building blocks of the dimer esters formed ~~by-through~~ β -pinene ozonolysis are attributed to one of the dicarboxylic acids, such as $C_9H_{14}O_4$ (*cis*-pinic acid), $C_8H_{12}O_4$ (*cis*-norpinic acid), and $C_8H_{14}O_5$ (diaterpenylic acid), which can be ~~well~~ ~~characterization indicators~~ of pinene oxidation products during dimer formation (Kenseth et al., 2018)-(Kenseth et al., 2018b). ~~Trimer-like compounds and highly oxidized dimers are typically in the range of 450~~ ~~~~~ ~~650 Da~~ (Kundu et al., 2012), with limonene SOA having a higher ~~RA~~ ~~relative abundance~~ than β -pinene SOA ~~as shown~~ ~~in~~ (Figure 4). The formation of trimers is associated with the presence of two double bonds in limonene. One of the C=C double bonds is first oxidized to the dimer products, while the ~~other~~ double bond ~~of the other~~ provides a reaction ~~point position~~ for further oxidation of the dimers, making it easier to form dimer RO₂ radicals (Guo et al., 2022). It is noticeable that the mechanism of dimer formation in similar monoterpene systems remains unresolved and warranty follow up studies (Kenseth et al., 2018)-(Kenseth et al., 2018b).

Formatted: Font color: Blue

Formatted: Font color: Blue

Formatted: Font color: Blue

Formatted: Font color: Blue

4 Conclusions

600 ~~The composition of aerosols varies systematically with gas-particle partitioning.~~ At lower mass concentrations, polar components seem to dominate the ~~organic~~ aerosols, while at higher concentrations, VOCs may condense (Grieshop et al., 2007). Environmental SOA ~~components compositions are considered to be~~ concentration-dependent, in agreement with the results of this ~~paper study~~. ~~Distribution of HOMs in SOA formed by ozonolysis oxidation are is~~ also affected ~~differently~~ by ozone concentrations. The precursors of β -pinene and limonene have the same molecular formula but different structures, ~~with~~ ~~with and with~~ β -pinene ~~was to be found to be~~ more obviously affected. The ~~relative abundance of HOMs~~ (RA_{HOMs}) in β -pinene SOA was more significantly affected by ozone concentration, while ~~that of~~ limonene SOA was ~~less almost hardly~~ weakly affected by ozone concentration, which was related to the high reactivity of limonene ~~with via~~ two double bonds and endocyclic structure. β -pinene was found more ~~inclined-prone~~ to form ~~the HOM~~ monomers ~~with~~ (C_8) and dimers ~~with~~ (C_{17} ~~fragments~~) ~~of~~ ~~HOMs~~, while limonene was more inclined to form HOMs monomers ~~with~~ (C_{10}) and dimers ~~with~~ (C_{19} ~~subgroups~~), which is ~~obviously related~~ ~~related~~ to the ~~way of broken bonds after ozone oxidation~~ ~~loss of a formaldehyde and subsequent oxidation of~~ ~~β -pinene by the addition of O₃ to the exocyclic double bond~~. In addition, distinct volatilities and abundances of HOMs in β -pinene and limonene SOA reflects the different molecular response of particulate reaction products to biogenic precursor oxidation ~~states~~, leading to different SOA size and number ~~concentration~~ distribution profiles. Higher ozone concentrations (315 ~~ppb~~ and 565 ppb) were favorable for the formation of HOMs and ELVOCs, and the number of unique organic molecules was higher. Compared ~~to with~~ β -pinene SOA, the abundance of ELVOCs in limonene SOA ~~contributes more is~~ higher.

Formatted: Font color: Blue

Formatted: Font color: Blue

Formatted: Font color: Blue

In addition to ~~the effect of ozone concentration on HOMs~~, other oxidants in the atmosphere may also have different effects impact the formation and evolution of ~~on~~ HOMs ~~them~~. For example, NO₂ inhibited the formation of highly oxidized dimer products by suppression of autoxidation (Rissanen, 2018). When considerable amount of 'OH was present, the potential dimer sources were can also be suppressed (Zhang et al., 2017). Moreover, Simon et al. (2020) found a continuously decreased in the oxidation level of α -pinene SOA and yields of HOMs as the temperature decreased from 25 to -50 °C (Simon et al., 2020). Similar result was also confirmed in urban field samples (Brean et al., 2020). Whether O₃ can exhibit a synergistic effect with other different oxidants and environmental conditions (e.g., humidity and temperature) in influencing HOMs formation and evolution is worthy to be explored in follow up studies. Current mass spectrometry techniques can only obtain information on the molecular formula of the HOMs, hindering the study of the detailed formation mechanism of many atmospheric precursors. Therefore, experimental conditions and new analytical techniques need to be developed to characterize HOMs rapidly and in detail. (Bianchi et al., 2019).

Data availability. The dataset for this paper is available upon request from the corresponding author (fupingqing@tju.edu.cn).
Author contribution. DL participated in the investigation, methodology, software development, formal analysis, and writing of the original draft. SZ and SC participated in the methodology and formal analysis. YZ collected the samples. All co-authors participated in validation as well as in reviewing and editing of the manuscript. PF and HT participated in the conceptualization, project administration, and funding acquisition.

Competing interests. The authors declare that they have no conflict of interests.

Acknowledgments. This work was supported by the National Natural Science Foundation of China (NSFC) (Grant Nos. 42130513 and 41625014), Tianjin Research Innovation Project for Postgraduate Students (Grant No. 2021YJSB135), Max Planck Institute for Chemistry, and Helmholtz-Zentrum Hereon. The authors thank Ulrich Pöschl for stimulating discussions.

References

- Atkinson, R. and Arey, J.: Atmospheric degradation of volatile organic compounds, Chem. Rev., 103, 4605-4638, <https://doi.org/10.1021/cr0206420>, 2003.
- Atkinson, R., Aschmann, S. M., Arey, J., and Shorees, B.: Formation of OH radicals in the gas phase reactions of O₃ with a series of terpenes, J. Geophys. Res., 97, 6065-6073, <https://doi.org/10.1029/92JD00062>, 1992.
- Badali, K. M., Zhou, S., Aljawhary, D., Antiñolo, M., Chen, W. J., Lok, A., Mungall, E., Wong, J. P. S., Zhao, R., and Abbatt, J. P. D.: Formation of hydroxyl radicals from photolysis of secondary organic aerosol material, Atmos. Chem. Phys., 15, 7831-7840, <https://doi.org/10.5194/acp-15-7831-2015>, 2015.
- Barsanti, K. C., Kroll, J. H., and Thornton, J. A.: Formation of low-volatility organic compounds in the atmosphere: Recent advancements and insights, J. Phys. Chem. Lett., 8, 1503-1511, <https://doi.org/10.1021/acs.jpcclett.6b02969>, 2017.
- Berndt, T., Mentler, B., Scholz, W., Fischer, L., Herrmann, H., Kulmala, M., and Hansel, A.: Accretion product formation from ozonolysis and OH radical reaction of α -pinene: Mechanistic insight and the influence of isoprene and ethylene, Environ. Sci. Technol., 52, 11069-11077, <https://doi.org/10.1021/acs.est.8b02210>, 2018a.
- Berndt, T., Scholz, W., Mentler, B., Fischer, L., Herrmann, H., Kulmala, M., and Hansel, A.: Accretion product formation from self- and cross-reactions of RO₂ radicals in the atmosphere, Angew. Chem. Int. Ed., 57, 3820-3824, <https://doi.org/10.1002/anie.201710989>, 2018b.
- Berndt, T., Richters, S., Jokinen, T., Hyttinen, N., Kurtén, T., Otkjær, R. V., Kjaergaard, H. G., Stratmann, F., Herrmann, H., Sipilä, M., Kulmala, M., and Ehn, M.: Hydroxyl radical-induced formation of highly oxidized organic compounds, Nat. Commun., 7, 13677,

Formatted: Font color: Blue

Formatted: Font color: Blue

Formatted: Font color: Blue

Formatted: Font color: Blue

Formatted: Font color: Blue

<https://doi.org/10.1038/ncomms13677>, 2016.

Bianchi, F., Kurten, T., Riva, M., Mohr, C., Rissanen, M. P., Roldin, P., Berndt, T., Crouse, J. D., Wennberg, P. O., Mentel, T. F., Wildt, J., Junninen, H., Jokinen, T., Kulmala, M., Worsnop, D. R., Thornton, J. A., Donahue, N., Kjaergaard, H. G., and Ehn, M.: Highly oxygenated organic molecules (HOM) from gas-phase autoxidation involving peroxy radicals: A key contributor to atmospheric aerosol, *Chem. Rev.*, 119, 3472-3509, <https://doi.org/10.1021/acs.chemrev.8b00395>, 2019.

Bianco, A., Deguillaume, L., Vaitilingom, M., Nicol, E., Baray, J. L., Chaumerliac, N., and Bridoux, M.: Molecular characterization of cloud water samples collected at the Puy de Dome (France) by Fourier transform ion cyclotron resonance mass spectrometry, *Environ. Sci. Technol.*, 52, 10275-10285, <https://doi.org/10.1021/acs.est.8b01964>, 2018.

Brean, J., Harrison, R. M., Shi, Z., Beddows, D. C. S., Acton, W. J. F., Hewitt, C. N., Squires, F. A., and Lee, J.: Observations of highly oxidized molecules and particle nucleation in the atmosphere of Beijing, *Atmos. Chem. Phys.*, 19, 14933-14947, <https://doi.org/10.5194/acp-19-14933-2019>, 2019.

Brean, J., Beddows, D. C. S., Shi, Z., Temime-Roussel, B., Marchand, N., Querol, X., Alastuey, A., Minguillón, M. C., and Harrison, R. M.: Molecular insights into new particle formation in Barcelona, Spain, *Atmos. Chem. Phys.*, 20, 10029-10045, <https://doi.org/10.5194/acp-20-10029-2020>, 2020.

Cao, D., Lv, J., Geng, F., Rao, Z., Niu, H., Shi, Y., Cai, Y., and Kang, Y.: Ion accumulation time dependent molecular characterization of natural organic matter using electrospray ionization-Fourier transform ion cyclotron resonance mass spectrometry, *Anal. Chem.*, 88, 12210-12218, <https://doi.org/10.1021/acs.analchem.6b03198>, 2016.

Chen, Q., Liu, Y., Donahue, N. M., Shilling, J. E., and Martin, S. T.: Particle-phase chemistry of secondary organic material: Modeled compared to measured O:C and H:C elemental ratios provide constraints, *Environ. Sci. Technol.*, 45, 4763-4770, <https://doi.org/10.1021/es104398g>, 2011.

Claffin, M. S., Krechmer, J. E., Hu, W., Jimenez, J. L., and Ziemann, P. J.: Functional group composition of secondary organic aerosol formed from ozonolysis of α -pinene under high VOC and autoxidation conditions, *ACS Earth Space Chem.*, 2, 1196-1210, <https://doi.org/10.1021/acsearthspacechem.8b00117>, 2018.

Cohen, A. J., Brauer, M., Burnett, R., Anderson, H. R., Frostad, J., Estep, K., Balakrishnan, K., Brunekreef, B., Dandona, L., Dandona, R., Feigin, V., Freedman, G., Hubbell, B., Jobling, A., Kan, H., Knibbs, L., Liu, Y., Martin, R., Morawska, L., Pope, C. A., Shin, H., Straif, K., Shaddick, G., Thomas, M., van Dingenen, R., van Donkelaar, A., Vos, T., Murray, C. J. L., and Forouzanfar, M. H.: Estimates and 25-year trends of the global burden of disease attributable to ambient air pollution: an analysis of data from the Global Burden of Diseases Study 2015, *The Lancet*, 389, 1907-1918, [https://doi.org/10.1016/S0140-6736\(17\)30505-6](https://doi.org/10.1016/S0140-6736(17)30505-6), 2017.

Crouse, J. D., Nielsen, L. B., Jørgensen, S., Kjaergaard, H. G., and Wennberg, P. O.: Autoxidation of organic compounds in the atmosphere, *J. Phys. Chem. Lett.*, 4, 3513-3520, <https://doi.org/10.1021/jz4019207>, 2013.

Donahue, N. M., Epstein, S. A., Pandis, S. N., and Robinson, A. L.: A two-dimensional volatility basis set: 1. organic-aerosol mixing thermodynamics, *Atmos. Chem. Phys.*, 11, 3303-3318, <https://doi.org/10.5194/acp-11-3303-2011>, 2011.

Donahue, N. M., Kroll, J. H., Pandis, S. N., and Robinson, A. L.: A two-dimensional volatility basis set – Part 2: Diagnostics of organic-aerosol evolution, *Atmos. Chem. Phys.*, 12, 615-634, <https://doi.org/10.5194/acp-12-615-2012>, 2012.

Ehn, M., Kleist, E., Junninen, H., Petäjä, T., Lönn, G., Schobesberger, S., Dal Maso, M., Trimborn, A., Kulmala, M., Worsnop, D. R., Wahner, A., Wildt, J., and Mentel, T. F.: Gas phase formation of extremely oxidized pinene reaction products in chamber and ambient air, *Atmos. Chem. Phys.*, 12, 5113-5127, <https://doi.org/10.5194/acp-12-5113-2012>, 2012.

Ehn, M., Thornton, J. A., Kleist, E., Sipila, M., Junninen, H., Pullinen, I., Springer, M., Rubach, F., Tillmann, R., Lee, B., Lopez-Hilfiker, F., Andres, S., Acir, I. H., Rissanen, M., Jokinen, T., Schobesberger, S., Kangasluoma, J., Kontkanen, J., Nieminen, T., Kurten, T., Nielsen, L. B., Jørgensen, S., Kjaergaard, H. G., Canagaratna, M., Maso, M. D., Berndt, T., Petaja, T., Wahner, A., Kerminen, V. M., Kulmala, M., Worsnop, D. R., Wildt, J., and Mentel, T. F.: A large source of low-volatility secondary organic aerosol, *Nature*, 506, 476-479, <https://doi.org/10.1038/nature13032>, 2014.

Fu, P., Kawamura, K., Chen, J., and Barrie, L. A.: Isoprene, monoterpene, and sesquiterpene oxidation products in the high Arctic aerosols during late winter to early summer, *Environ. Sci. Technol.*, 43, 4022-4028, <https://doi.org/10.1021/es803669a>, 2009.

Gallimore, P. J., Mahon, B. M., Wragg, F. P. H., Fuller, S. J., Giorio, C., Kourchev, I., and Kalberer, M.: Multiphase composition changes and reactive oxygen species formation during limonene oxidation in the new Cambridge Atmospheric Simulation Chamber (CASC), *Atmos. Chem. Phys.*, 17, 9853-9868, <https://doi.org/10.5194/acp-17-9853-2017>, 2017.

Gong, Y., Chen, Z., and Li, H.: The oxidation regime and SOA composition in limonene ozonolysis: roles of different double bonds, radicals, and water, *Atmos. Chem. Phys.*, 18, 15105-15123, <https://doi.org/10.5194/acp-18-15105-2018>, 2018.

Grieshop, A. P., Donahue, N. M., and Robinson, A. L.: Is the gas-particle partitioning in alpha-pinene secondary organic aerosol reversible?, *Geophys. Res. Lett.*, 34, L14810, <https://doi.org/10.1029/2007gl029987>, 2007.

Griffin, R. J., Cocker, D. R., Flagan, R. C., and Seinfeld, J. H.: Organic aerosol formation from the oxidation of biogenic hydrocarbons, *J. Geophys. Res.-Atmos.*, 104, 3555-3567, <https://doi.org/10.1029/1998jd100049>, 1999.

Guenther, A. B., Jiang, X., Heald, C. L., Sakulyanontvittaya, T., Duhl, T., Emmons, L. K., and Wang, X.: The model of emissions of Gases and Aerosols from Nature version 2.1 (MEGAN2.1): An extended and updated framework for modeling biogenic emissions, *Geosci. Model Dev.*, 5, 1471-1492, <https://doi.org/10.5194/gmd-5-1471-2012>, 2012.

Formatted: Font color: Blue

Formatted: Font color: Blue

Formatted: Font color: Blue

Formatted: Font color: Blue

Formatted: Font color: Blue

Formatted: Font color: Blue

Formatted: Font color: Blue

Formatted: Font color: Blue

Formatted: Font color: Blue

710 Guo, Y., Shen, H., Pullinen, I., Luo, H., Kang, S., Vereecken, L., Fuchs, H., Hallquist, M., Acir, I.-H., Tillmann, R., Rohrer, F., Wildt, J.,
 Kiendler-Scharr, A., Wahner, A., Zhao, D., and Mentel, T. F.: Identification of highly oxygenated organic molecules and their role in aerosol
 formation in the reaction of limonene with nitrate radical, *Atmos. Chem. Phys.*, 22, 11323-11346, [https://doi.org/10.5194/acp-22-11323-](https://doi.org/10.5194/acp-22-11323-2022)
[2022](https://doi.org/10.5194/acp-22-11323-2022), 2022.

715 Hallquist, M., Wenger, J. C., Baltensperger, U., Rudich, Y., Simpson, D., Claeys, M., Dommen, J., Donahue, N. M., George, C., Goldstein,
 A. H., Hamilton, J. F., Herrmann, H., Hoffmann, T., Iinuma, Y., Jang, M., Jenkin, M. E., Jimenez, J. L., Kiendler-Scharr, A., Maenhaut, W.,
 McFiggans, G., Mentel, T. F., Monod, A., Prévôt, A. S. H., Seinfeld, J. H., Surratt, J. D., Szmigielski, R., and Wildt, J.: The formation,
 properties and impact of secondary organic aerosol: current and emerging issues, *Atmos. Chem. Phys.*, 9, 5155-5236,
<https://doi.org/10.5194/acp-9-5155-2009>, 2009.

720 Hammes, J., Lutz, A., Mentel, T., Faxon, C., and Hallquist, M.: Carboxylic acids from limonene oxidation by ozone and hydroxyl radicals:
 insights into mechanisms derived using a FIGAERO-CIMS, *Atmos. Chem. Phys.*, 19, 13037-13052, [https://doi.org/10.5194/acp-19-13037-](https://doi.org/10.5194/acp-19-13037-2019)
[2019](https://doi.org/10.5194/acp-19-13037-2019), 2019.

725 Iyer, S., Rissanen, M. P., Valiev, R., Barua, S., Krechmer, J. E., Thornton, J., Ehn, M., and Kurten, T.: Molecular mechanism for rapid
 autoxidation in α -pinene ozonolysis, *Nat. Commun.*, 12, 878, <https://doi.org/10.1038/s41467-021-21172-w>, 2021.

730 Jaoui, M. and Kamens, R. M.: Gaseous and particulate oxidation products analysis of a mixture of α -pinene + β -pinene/O₃/air in the absence
 of light and α -pinene + β -pinene/NO_x/air in the presence of natural sunlight, *J. Atmos. Chem.*, 44, 259-297,
<https://doi.org/10.1023/A:1022977427523>, 2003.

735 Jokinen, T., Sipilä, M., Richters, S., Kerminen, V.-M., Paasonen, P., Stratmann, F., Worsnop, D., Kulmala, M., Ehn, M., Herrmann, H., and
 Berndt, T.: Rapid autoxidation forms highly oxidized RO₂ radicals in the atmosphere, *Angew. Chem. Int. Ed. Engl.*, 53, 14596-14600,
<https://doi.org/10.1002/anie.201408566>, 2014.

740 Jokinen, T., Berndt, T., Makkonen, R., Kerminen, V. M., Junninen, H., Paasonen, P., Stratmann, F., Herrmann, H., Guenther, A. B., Worsnop,
 D. R., Kulmala, M., Ehn, M., and Sipilä, M.: Production of extremely low volatile organic compounds from biogenic emissions: Measured
 yields and atmospheric implications, *Proc. Natl. Acad. Sci. USA*, 112, 7123-7128, <https://doi.org/10.1073/pnas.1423977112>, 2015.

745 Kahnt, A., Vermeylen, R., Iinuma, Y., Safi Shalamzari, M., Maenhaut, W., and Claeys, M.: High-molecular-weight esters in α -pinene
 ozonolysis secondary organic aerosol: structural characterization and mechanistic proposal for their formation from highly oxygenated
 molecules, *Atmos. Chem. Phys.*, 18, 8453-8467, <https://doi.org/10.5194/acp-18-8453-2018>, 2018.

750 [Kamens, R., Jang, M., Chien, C.-J., and Leach, K.: Aerosol formation from the reaction of \$\alpha\$ -pinene and ozone using a gas-phase kinetics-](https://doi.org/10.5194/acp-5-1053-2005)
[aerosol partitioning model, *Environ. Sci. Technol.*, 33, 1430-1438, <https://doi.org/10.1021/es980725r>, 1999.](https://doi.org/10.5194/acp-5-1053-2005)

755 Kanakidou, M., Seinfeld, J. H., Pandis, S. N., Barnes, I., Dentener, F. J., Facchini, M. C., Van Dingenen, R., Ervens, B., Nenes, A., Nielsen,
 C. J., Swietlicki, E., Putaud, J. P., Balkanski, Y., Fuzzi, S., Horth, J., Moortgat, G. K., Winterhalter, R., Myhre, C. E. L., Tsigaridis, K., Vignati,
 E., Stephanou, E. G., and Wilson, J.: Organic aerosol and global climate modelling: a review, *Atmos. Chem. Phys.*, 5, 1053-1123,
<https://doi.org/10.5194/acp-5-1053-2005>, 2005.

760 Kenseth, C. M., Huang, Y., Zhao, R., Dalleska, N. F., Hethcox, J. C., Stoltz, B. M., and Seinfeld, J. H.: Synergistic O₃ + OH oxidation
 pathway to extremely low-volatility dimers revealed in β -pinene secondary organic aerosol, *Proc. Natl. Acad. Sci. USA*, 115, 8301-8306,
<https://doi.org/10.1073/pnas.1804671115>, 2018.

765 Kerminen, V. M., Paramonov, M., Anttila, T., Riipinen, I., Fountoukis, C., Korhonen, H., Asmi, E., Laakso, L., Lihavainen, H., Swietlicki,
 E., Svenningsson, B., Asmi, A., Pandis, S. N., Kulmala, M., and Petäjä, T.: Cloud condensation nuclei production associated with atmospheric
 nucleation: a synthesis based on existing literature and new results, *Atmos. Chem. Phys.*, 12, 12037-12059, [https://doi.org/10.5194/acp-12-](https://doi.org/10.5194/acp-12-12037-2012)
[12037-2012](https://doi.org/10.5194/acp-12-12037-2012), 2012.

770 Kirkby, J., Duplissy, J., Sengupta, K., Frege, C., Gordon, H., Williamson, C., Heinritzi, M., Simon, M., Yan, C., Almeida, J., Trostl, J.,
 Nieminen, T., Ortega, I. K., Wagner, R., Adamov, A., Amorim, A., Bernhammer, A. K., Bianchi, F., Breitenlechner, M., Brilke, S., Chen, X.,
 Craven, J., Dias, A., Ehrhart, S., Flagan, R. C., Franchin, A., Fuchs, C., Guida, R., Hakala, J., Hoyle, C. R., Jokinen, T., Junninen, H.,
 Kangasluoma, J., Kim, J., Krapf, M., Kurten, A., Laaksonen, A., Lehtipalo, K., Makhmutov, V., Mathot, S., Molteni, U., Onnela, A., Perakyla,
 O., Piel, F., Petaja, T., Praplan, A. P., Pringle, K., Rap, A., Richards, N. A., Riipinen, I., Rissanen, M. P., Rondo, L., Sarnela, N., Schobesberger,
 S., Scott, C. E., Seinfeld, J. H., Sipilä, M., Steiner, G., Stozhkov, Y., Stratmann, F., Tome, A., Virtanen, A., Vogel, A. L., Wagner, A. C.,
 Wagner, P. E., Weingartner, E., Wimmer, D., Winkler, P. M., Ye, P., Zhang, X., Hansel, A., Dommen, J., Donahue, N. M., Worsnop, D. R.,
 Baltensperger, U., Kulmala, M., Carslaw, K. S., and Curtius, J.: Ion-induced nucleation of pure biogenic particles, *Nature*, 533, 521-526,
<https://doi.org/10.1038/nature17953>, 2016.

775 Koch, B. P., Dittmar, T., Witt, M., and Kattner, G.: Fundamentals of molecular formula assignment to ultrahigh resolution mass data of
 natural organic matter, *Anal. Chem.*, 79, 1758-1763, <https://doi.org/10.1021/ac061949s>, 2007.

780 Koch, B. P., Witt, M., Engbrodt, R., Dittmar, T., and Kattner, G.: Molecular formulae of marine and terrigenous dissolved organic matter
 detected by electrospray ionization Fourier transform ion cyclotron resonance mass spectrometry, *Geochim. Cosmochim. Ac.*, 69, 3299-
 3308, <https://doi.org/10.1016/j.gca.2005.02.027>, 2005.

785 Kourtchev, I., Giorio, C., Manninen, A., Wilson, E., Mahon, B., Aalto, J., Kajos, M., Venables, D., Ruuskanen, T., Levula, J., Loponen, M.,
 Connors, S., Harris, N., Zhao, D., Kiendler-Scharr, A., Mentel, T., Rudich, Y., Hallquist, M., Doussin, J.-F., Maenhaut, W., Bäck, J., Petäjä,
 T., Wenger, J., Kulmala, M., and Kalberer, M.: Enhanced Volatile Organic Compounds emissions and organic aerosol mass increase the

Formatted: Font color: Blue

Formatted: Font color: Blue

Formatted: Font color: Blue

oligomer content of atmospheric aerosols, *Sci. Rep.*, 6, 35038, <https://doi.org/10.1038/srep35038>, 2016.

765 Kristensen, K., Watne, Å. K., Hammes, J., Lutz, A., Petäjä, T., Hallquist, M., Bilde, M., and Glasius, M.: High-molecular weight dimer esters are major products in aerosols from α -pinene ozonolysis and the boreal forest, *Environ. Sci. Technol. Lett.*, 3, 280-285, <https://doi.org/10.1021/acs.estlett.6b00152>, 2016.

Kroll, J. H. and Seinfeld, J. H.: Chemistry of secondary organic aerosol: Formation and evolution of low-volatility organics in the atmosphere, *Atmos. Environ.*, 42, 3593-3624, <https://doi.org/10.1016/j.atmosenv.2008.01.003>, 2008.

770 Kroll, J. H., Donahue, N. M., Jimenez, J. L., Kessler, S. H., Canagaratna, M. R., Wilson, K. R., Altieri, K. E., Mazzoleni, L. R., Wozniak, A. S., Bluhm, H., Mysak, E. R., Smith, J. D., Kolb, C. E., and Worsnop, D. R.: Carbon oxidation state as a metric for describing the chemistry of atmospheric organic aerosol, *Nat. Chem.*, 3, 133-139, <https://doi.org/10.1038/nchem.948>, 2011.

Kundu, S., Fisscha, R., Putman, A. L., Rahn, T. A., and Mazzoleni, L. R.: High molecular weight SOA formation during limonene ozonolysis: insights from ultrahigh-resolution FT-ICR mass spectrometry characterization, *Atmos. Chem. Phys.*, 12, 5523-5536, <https://doi.org/10.5194/acp-12-5523-2012>, 2012.

775 Laden, F., Schwartz, J., Speizer, F. E., and Dockery, D. W.: Reduction in fine particulate air pollution and mortality, *Am. J. Resp. Crit. Care*, 173, 667-672, <https://doi.org/10.1164/rccm.200503-443OC>, 2006.

Lee, R., Gryn'ova, G., Ingold, K. U., and Cooto, M. L.: Why are sec-alkylperoxyl bimolecular self-reactions orders of magnitude faster than the analogous reactions of tert-alkylperoxyls? The unanticipated role of CH hydrogen bond donation, *Phys. Chem. Chem. Phys.*, 18, 23673-23679, <https://doi.org/10.1039/c9cp04670c>, 2016.

780 Li, H., Yang, Y., Jin, J., Wang, H., Li, K., Wang, P., and Liao, H.: Climate-driven deterioration of future ozone pollution in Asia predicted by machine learning with multi-source data, *Atmos. Chem. Phys.*, 23, 1131-1145, <https://doi.org/10.5194/acp-23-1131-2023>, 2023.

Li, M., Li, J., Zhu, Y., Chen, J., Andreae, M. O., Pöschl, U., Su, H., Kulmala, M., Chen, C., Cheng, Y., and Zhao, J.: Highly oxygenated organic molecules with high unsaturation formed upon photochemical aging of soot, *Chem.*, 8, 2688-2699, <https://doi.org/10.1016/j.chempr.2022.06.011>, 2022.

785 Li, X., Chee, S., Hao, J., Abbott, J. P. D., Jiang, J., and Smith, J. N.: Relative humidity effect on the formation of highly oxidized molecules and new particles during monoterpene oxidation, *Atmos. Chem. Phys.*, 19, 1555-1570, <https://doi.org/10.5194/acp-19-1555-2019>, 2019.

Li, Y., Pöschl, U., and Shiraiwa, M.: Molecular corridors and parameterizations of volatility in the chemical evolution of organic aerosols, *Atmos. Chem. Phys.*, 16, 3327-3344, <https://doi.org/10.5194/acp-16-3327-2016>, 2016.

790 Liu, P., Li, Y. J., Wang, Y., Gilles, M. K., Zaveri, R. A., Bertram, A. K., and Martin, S. T.: Lability of secondary organic particulate matter, *Proc. Natl. Acad. Sci. USA*, 113, 12643-12648, <https://doi.org/10.1073/pnas.1603138113>, 2016.

Ma, Y. and Marston, G.: Multifunctional acid formation from the gas-phase ozonolysis of β -pinene, *Phys. Chem. Chem. Phys.*, 10, 6115-6126, <https://doi.org/10.1039/b807863g>, 2008.

Mahilang, M., Deb, M. K., and Pervez, S.: Biogenic secondary organic aerosols: A review on formation mechanism, analytical challenges and environmental impacts, *Chemosphere*, 262, 127771, <https://doi.org/10.1016/j.chemosphere.2020.127771>, 2021.

795 Molteni, U., Bianchi, F., Klein, F., El Haddad, I., Frege, C., Rossi, M. J., Dommen, J., and Baltensperger, U.: Formation of highly oxygenated organic molecules from aromatic compounds, *Atmos. Chem. Phys.*, 18, 1909-1921, <https://doi.org/10.5194/acp-18-1909-2018>, 2018.

Mutzel, A., Rodigast, M., Inuma, Y., Böge, O., and Herrmann, H.: Monoterpene SOA – contribution of first-generation oxidation products to formation and chemical composition, *Atmos. Environ.*, 130, 136-144, <https://doi.org/10.1016/j.atmosenv.2015.10.080>, 2016.

800 Noziere, B., Kalberer, M., Claeys, M., Allan, J., D'Anna, B., Decesari, S., Finessi, E., Glasius, M., Grgic, I., Hamilton, J. F., Hoffmann, T., Inuma, Y., Jaoui, M., Kahnt, A., Kampf, C. J., Kourtev, I., Maenhaut, W., Marsden, N., Saarikoski, S., Schnelle-Kreis, J., Surratt, J. D., Szidat, S., Szmigielski, R., and Wisthaler, A.: The molecular identification of organic compounds in the atmosphere: state of the art and challenges, *Chem. Rev.*, 115, 3919-3983, <https://doi.org/10.1021/cr5003485>, 2015.

Pathak, R., Donahue, N. M., and Pandis, S. N.: Ozonolysis of β -Pinene: Temperature dependence of secondary organic aerosol mass fraction, *Environ. Sci. Technol.*, 42, 5081-5086, <https://doi.org/10.1021/es070721z>, 2008.

805 Pathak, R. K., Salo, K., Emanuelsson, E. U., Cai, C., Lutz, A., Hallquist, A. M., and Hallquist, M.: Influence of ozone and radical chemistry on limonene organic aerosol production and thermal characteristics, *Environ. Sci. Technol.*, 46, 11660-11669, <https://doi.org/10.1021/es301750r>, 2012.

Peräkylä, O., Riva, M., Heikkinen, L., Quéléver, L., Roldin, P., and Ehn, M.: Experimental investigation into the volatilities of highly oxygenated organic molecules (HOMs), *Atmos. Chem. Phys.*, 20, 649-669, <https://doi.org/10.5194/acp-20-649-2020>, 2020.

810 Perraud, V., Bruns, E. A., Ezell, M. J., Johnson, S. N., Yu, Y., Alexander, M. L., Zelenyuk, A., Imre, D., Chang, W. L., Dabdub, D., Pankov, J. F., and Finlayson-Pitts, B. J.: Nonequilibrium atmospheric secondary organic aerosol formation and growth, *Proc. Natl. Acad. Sci. USA*, 109, 2836-2841, <https://doi.org/10.1073/pnas.1119909109>, 2012.

Pullinen, I., Schmitt, S., Kang, S., Sarrafzadeh, M., Schlag, P., Andres, S., Kleist, E., Mentel, T. F., Rohrer, F., Springer, M., Tillmann, R., Wildt, J., Wu, C., Zhao, D., Wahner, A., and Kiendler-Scharr, A.: Impact of NO_x on secondary organic aerosol (SOA) formation from α -pinene and β -pinene photooxidation: the role of highly oxygenated organic nitrates, *Atmos. Chem. Phys.*, 20, 10125-10147, <https://doi.org/10.5194/acp-20-10125-2020>, 2020.

815 Ramanathan, V., Crutzen, P. J., Kiehl, J. T., and Rosenfeld, D.: Aerosols, climate, and the hydrological cycle, *Science*, 294, 2119-2124, <https://doi.org/10.1126/science.1064034>, 2001.

Formatted: Font color: Blue

Formatted: Font color: Blue

Formatted: Font color: Blue

Formatted: Font color: Blue

Formatted: Font color: Blue

Formatted: Font color: Blue

Formatted: Font color: Blue

Formatted: Font color: Blue

Formatted: Font color: Blue

Formatted: Font color: Blue

820 Rissanen, M. P.: NO₂ suppression of autoxidation–inhibition of gas-phase highly oxidized dimer product formation, *ACS Earth Space Chem.*, 2, 1211-1219, <https://doi.org/10.1021/acsearthspacechem.8b00123>, 2018.

Rissanen, M. P., Kurtén, T., Sipilä, M., Thornton, J. A., Kangasluoma, J., Sarnela, N., Junninen, H., Jørgensen, S., Schallhart, S., Kajos, M. K., Taipale, R., Springer, M., Mentel, T. F., Ruuskanen, T., Petäjä, T., Worsnop, D. R., Kjaergaard, H. G., and Ehn, M.: The formation of highly oxidized multifunctional products in the ozonolysis of cyclohexene, *J. Am. Chem. Soc.*, 136, 15596-15606, <https://doi.org/10.1021/ja507146s>, 2014.

825 Rohr, A. C., Weschler, C. J., Koutrakis, P., and Spengler, J. D.: Generation and quantification of ultrafine particles through terpene/ozone reaction in a chamber setting, *Aerosol Sci. Technol.*, 37, 65-78, <https://doi.org/10.1080/02786820300892>, 2003.

Roldin, P., Ehn, M., Kurten, T., Olenius, T., Rissanen, M. P., Sarnela, N., Elm, J., Rantala, P., Hao, L., Hyttinen, N., Heikkinen, L., Worsnop, D. R., Pichelstorfer, L., Xavier, C., Clusius, P., Ostrom, E., Petaja, T., Kulmala, M., Vehkamäki, H., Virtanen, A., Riipinen, I., and Boy, M.: The role of highly oxygenated organic molecules in the boreal aerosol-cloud-climate system, *Nat. Commun.*, 10, 4370, <https://doi.org/10.1038/s41467-019-12338-8>, 2019.

830 Saukko, E., Lambe, A. T., Massoli, P., Koop, T., Wright, J. P., Croasdale, D. R., Pedernera, D. A., Onasch, T. B., Laaksonen, A., Davidovits, P., Worsnop, D. R., and Virtanen, A.: Humidity-dependent phase state of SOA particles from biogenic and anthropogenic precursors, *Atmos. Chem. Phys.*, 12, 7517-7529, <https://doi.org/10.5194/acp-12-7517-2012>, 2012.

Schervish, M. and Donahue, N. M.: Peroxy radical chemistry and the volatility basis set, *Atmos. Chem. Phys.*, 20, 1183-1199, <https://doi.org/10.5194/acp-20-1183-2020>, 2020.

835 Shah, R. U., Coggon, M. M., Gkatzelis, G. I., McDonald, B. C., Tasoglou, A., Huber, H., Gilman, J., Warneke, C., Robinson, A. L., and Presto, A. A.: Urban oxidation flow reactor measurements reveal significant secondary organic aerosol contributions from volatile emissions of emerging importance, *Environ. Sci. Technol.*, 54, 714-725, <https://doi.org/10.1021/acs.est.9b06531>, 2019.

840 Shen, H., Zhao, D., Pullinen, I., Kang, S., Vereecken, L., Fuchs, H., Acir, I. H., Tillmann, R., Rohrer, F., Wildt, J., Kiendler-Scharr, A., Wahner, A., and Mentel, T. F.: Highly oxygenated organic nitrates formed from NO₃ radical-initiated oxidation of β-pinene, *Environ. Sci. Technol.*, 55, 15658-15671, <https://doi.org/10.1021/acs.est.1c03978>, 2021.

Shi, X., Tang, R., Dong, Z., Liu, H., Xu, F., Zhang, Q., Zong, W., and Cheng, J.: A neglected pathway for the accretion products formation in the atmosphere, *Sci. Total Environ.*, 848, 157494, <https://doi.org/10.1016/j.scitotenv.2022.157494>, 2022.

845 Shiraiwa, M., Berkemeier, T., Schilling-Fahnestock, K. A., Seinfeld, J. H., and Pöschl, U.: Molecular corridors and kinetic regimes in the multiphase chemical evolution of secondary organic aerosol, *Atmos. Chem. Phys.*, 14, 8323-8341, <https://doi.org/10.5194/acp-14-8323-2014>, 2014.

Shrivastava, M., Cappa, C. D., Fan, J., Goldstein, A. H., Guenther, A. B., Jimenez, J. L., Kuang, C., Laskin, A., Martin, S. T., Ng, N. L., Petaja, T., Pierce, J. R., Rasch, P. J., Roldin, P., Seinfeld, J. H., Shilling, J., Smith, J. N., Thornton, J. A., Volkamer, R., Wang, J., Worsnop, D. R., Zaveri, R. A., Zelenyuk, A., and Zhang, Q.: Recent advances in understanding secondary organic aerosol: Implications for global climate forcing, *Rev. Geophys.*, 55, 509-559, <https://doi.org/10.1002/2016rg000540>, 2017.

850 Simon, M., Dada, L., Heinritzi, M., Scholz, W., Stolzenburg, D., Fischer, L., Wagner, A. C., Kürten, A., Rörup, B., He, X.-C., Almeida, J., Baalbaki, R., Baccarini, A., Bauer, P. S., Beck, L., Bergen, A., Bianchi, F., Bräkling, S., Brilke, S., Caudillo, L., Chen, D., Chu, B., Dias, A., Draper, D. C., Duplissy, J., El-Haddad, I., Finkenzeller, H., Frege, C., Gonzalez-Carracedo, L., Gordon, H., Granzin, M., Hakala, J., Hofbauer, V., Hoyle, C. R., Kim, C., Kong, W., Lamkaddam, H., Lee, C. P., Lehtipalo, K., Leiminger, M., Mai, H., Manninen, H. E., Marie, G., Marten, R., Mentler, B., Molteni, U., Nichman, L., Nie, W., Ojdanic, A., Onnela, A., Partoll, E., Petäjä, T., Pfeifer, J., Philippov, M., Quéléver, L. L. J., Ranjithkumar, A., Rissanen, M. P., Schallhart, S., Schobesberger, S., Schuchmann, S., Shen, J., Sipilä, M., Steiner, G., Stozhkov, Y., Tauber, C., Tham, Y. J., Tomé, A. R., Vazquez-Pufleau, M., Vogel, A. L., Wagner, R., Wang, M., Wang, D. S., Wang, Y., Weber, S. K., Wu, Y., Xiao, M., Yan, C., Ye, P., Ye, Q., Zauner-Wieczorek, M., Zhou, X., Baltensperger, U., Dommen, J., Flagan, R. C., Hansel, A., Kulmala, M., Volkamer, R., Winkler, P. M., Worsnop, D. R., Donahue, N. M., Kirkby, J., and Curtius, J.: Molecular understanding of new-particle formation from α-pinene between -50 and +25 °C, *Atmos. Chem. Phys.*, 20, 9183-9207, <https://doi.org/10.5194/acp-20-9183-2020>, 2020.

860 Song, C., Zaveri, R. A., Shilling, J. E., Alexander, M. L., and Newburn, M.: Effect of hydrophilic organic seed aerosols on secondary organic aerosol formation from ozonolysis of α-pinene, *Environ. Sci. Technol.*, 45, 7323-7329, <https://doi.org/10.1021/es201225c>, 2011.

Takekawa, H., Minoura, H., and Yamazaki, S.: Temperature dependence of secondary organic aerosol formation by photo-oxidation of hydrocarbons, *Atmos. Environ.*, 37, 3413-3424, [https://doi.org/10.1016/S1352-2310\(03\)00359-5](https://doi.org/10.1016/S1352-2310(03)00359-5), 2003.

865 Tomaz, S., Wang, D., Zabalegui, N., Li, D., Lamkaddam, H., Bachmeier, F., Vogel, A., Monge, M. E., Perrier, S., Baltensperger, U., George, C., Rissanen, M., Ehn, M., El Haddad, I., and Riva, M.: Structures and reactivity of peroxy radicals and dimeric products revealed by online tandem mass spectrometry, *Nat. Commun.*, 12, 300, <https://doi.org/10.1038/s41467-020-20532-2>, 2021.

Tong, H., Arangio, A. M., Lakey, P. S. J., Berkemeier, T., Liu, F., Kampf, C. J., Brune, W. H., Pöschl, U., and Shiraiwa, M.: Hydroxyl radicals from secondary organic aerosol decomposition in water, *Atmos. Chem. Phys.*, 16, 1761-1771, <https://doi.org/10.5194/acp-16-1761-2016>, 2016.

870 Tong, H., Lakey, P. S. J., Arangio, A. M., Socorro, J., Shen, F., Lucas, K., Brune, W. H., Pöschl, U., and Shiraiwa, M.: Reactive oxygen species formed by secondary organic aerosols in water and surrogate lung fluid, *Environ. Sci. Technol.*, 52, 11642-11651, <https://doi.org/10.1021/acs.est.8b03695>, 2018.

Tong, H., Zhang, Y., Filippi, A., Wang, T., Li, C., Liu, F., Leppla, D., Kourtchev, I., Wang, K., Keskinen, H.-M., Levula, J. T., Arangio, A.

Formatted: Font color: Blue

Formatted: Font color: Blue

Formatted: Font color: Blue

Formatted: Font color: Blue

Formatted: Font color: Blue

Formatted: Font color: Blue

Formatted: Font color: Blue

Formatted: Font color: Blue

Formatted: Font color: Blue

Formatted: Font color: Blue

Formatted: Font color: Blue

Formatted: Font color: Blue

Formatted: Font color: Blue

Formatted: Font color: Blue

Formatted: Font color: Blue

Formatted: Font color: Blue

Formatted: Font color: Blue

Formatted: Font color: Blue

- 875 M., Shen, F., Ditas, F., Martin, S. T., Artaxo, P., Godeoi, R. H. M., Yamamoto, C. I., de Souza, R. A. F., Huang, R.-J., Berkemeier, T., Wang, Y., Su, H., Cheng, Y., Pope, F. D., Fu, P., Yao, M., Pöhlker, C., Petäjä, T., Kulmala, M., Andreae, M. O., Shiraiwa, M., Pöschl, U., Hoffmann, T., and Kalberer, M.: Radical formation by fine particulate matter associated with highly oxygenated molecules, *Environ. Sci. Technol.*, **53**, 12506-12518, <https://doi.org/10.1021/acs.est.9b05149>, 2019.
- 880 Tröstl, J., Chuang, W. K., Gordon, H., Heinritzi, M., Yan, C., Molteni, U., Ahlm, L., Frege, C., Bianchi, F., Wagner, R., Simon, M., Lehtipalo, K., Williamson, C., Craven, J. S., Duplissy, J., Adamov, A., Almeida, J., Bernhammer, A.-K., Breitenlechner, M., Brilke, S., Dias, A., Ehrhart, S., Flagan, R. C., Franchin, A., Fuchs, C., Guida, R., Gysel, M., Hansel, A., Hoyle, C. R., Jokinen, T., Junninen, H., Kangasluoma, J., Keskinen, H., Kim, J., Krapf, M., Kürten, A., Laaksonen, A., Lawler, M., Leiminger, M., Mathot, S., Möhler, O., Nieminen, T., Onnela, A., Petäjä, T., Piel, F. M., Miettinen, P., Rissanen, M. P., Rondo, L., Sarnela, N., Schobesberger, S., Sengupta, K., Sipilä, M., Smith, J. N., Steiner, G., Tomé, A., Virtanen, A., Wagner, A. C., Weingartner, E., Wimmer, D., Winkler, P. M., Ye, P., Carslaw, K. S., Curtius, J., Dommen, J., Kirkby, J., Kulmala, M., Riipinen, I., Worsnop, D. R., Donahue, N. M., and Baltensperger, U.: The role of low-volatility organic compounds in initial particle growth in the atmosphere, *Nature*, **533**, 527-531, <https://doi.org/10.1038/nature18271>, 2016.
- 885 Tu, P., Hall, W. A. t., and Johnston, M. V.: Characterization of highly oxidized molecules in fresh and aged biogenic secondary organic aerosol, *Anal. Chem.*, **88**, 4495-4501, <https://doi.org/10.1021/acs.analchem.6b00378>, 2016.
- 890 Vogel, A. L., Schneider, J., Müller-Tautges, C., Klimach, T., and Hoffmann, T.: Aerosol chemistry resolved by mass spectrometry: Insights into particle growth after ambient new particle formation, *Environ. Sci. Technol.*, **50**, 10814-10822, <https://doi.org/10.1021/acs.est.6b01673>, 2016.
- Wang, L. and Wang, L.: The oxidation mechanism of gas-phase ozonolysis of limonene in the atmosphere, *Phys. Chem. Chem. Phys.*, **23**, 9294-9303, <https://doi.org/10.1039/d0cp05803c>, 2021.
- 895 Wang, M., Chen, D., Xiao, M., Ye, Q., Stolzenburg, D., Hofbauer, V., Ye, P., Vogel, A. L., Mauldin, R. L., 3rd, Amorim, A., Baccarini, A., Baumgartner, B., Brilke, S., Dada, L., Dias, A., Duplissy, J., Finkenzeller, H., Garmash, O., He, X. C., Hoyle, C. R., Kim, C., Kvashnin, A., Lehtipalo, K., Fischer, L., Molteni, U., Petaja, T., Pospisilova, V., Quelever, L. L. J., Rissanen, M., Simon, M., Tauber, C., Tome, A., Wagner, A. C., Weitz, L., Volkamer, R., Winkler, P. M., Kirkby, J., Worsnop, D. R., Kulmala, M., Baltensperger, U., Dommen, J., El-Haddad, I., and Donahue, N. M.: Photo-oxidation of aromatic hydrocarbons produces low-volatility organic compounds, *Environ. Sci. Technol.*, **54**, 7911-7921, <https://doi.org/10.1021/acs.est.0c02100>, 2020.
- 900 Wang, S., Zhao, Y., Chan, A. W. H., Yao, M., Chen, Z., and Abbatt, J. P. D.: Organic peroxides in aerosol: Key reactive intermediates for multiphase processes in the atmosphere, *Chem. Rev.*, **123**, 1635-1679, <https://doi.org/10.1021/acs.chemrev.2c00430>, 2023.
- Waring, M. S., Wells, J. R., and Siegel, J. A.: Secondary organic aerosol formation from ozone reactions with single terpenoids and terpenoid mixtures, *Atmos. Environ.*, **45**, 4235-4242, <https://doi.org/10.1016/j.atmosenv.2011.05.001>, 2011.
- 905 Wu, K., Yang, X., Chen, D., Gu, S., Lu, Y., Jiang, Q., Wang, K., Ou, Y., Qian, Y., Shao, P., and Lu, S.: Estimation of biogenic VOC emissions and their corresponding impact on ozone and secondary organic aerosol formation in China, *Atmos. Res.*, **231**, <https://doi.org/10.1016/j.atmosres.2019.104656>, 2020.
- Wu, Z., Rodgers, R. P., and Marshall, A. G.: Two- and three-dimensional van Krevelen diagrams: A graphical analysis complementary to the Kendrick mass plot for sorting elemental compositions of complex organic mixtures based on ultrahigh-resolution broadband Fourier transform ion cyclotron resonance mass measurements, *Anal. Chem.*, **76**, 2511-2516, <https://doi.org/10.1021/ac0355449>, 2004.
- 910 Xie, Q., Su, S., Dai, Y., Hu, W., Yue, S., Cao, D., Jiang, G., and Fu, P.: Deciphering ¹³C and ³⁴S isotopes of organosulfates in urban aerosols by FT-ICR mass spectrometry, *Environ. Sci. Technol. Lett.*, **9**, 526-532, <https://doi.org/10.1021/acs.estlett.2c00255>, 2022.
- Xie, Q., Su, S., Chen, S., Xu, Y., Cao, D., Chen, J., Ren, L., Yue, S., Zhao, W., Sun, Y., Wang, Z., Tong, H., Su, H., Cheng, Y., Kawamura, K., Jiang, G., Liu, C.-Q., and Fu, P.: Molecular characterization of firework-related urban aerosols using Fourier transform ion cyclotron resonance mass spectrometry, *Atmos. Chem. Phys.*, **20**, 6803-6820, <https://doi.org/10.5194/acp-20-6803-2020>, 2020a.
- 915 Xie, Q., Li, Y., Yue, S., Su, S., Cao, D., Xu, Y., Chen, J., Tong, H., Su, H., Cheng, Y., Zhao, W., Hu, W., Wang, Z., Yang, T., Pan, X., Sun, Y., Wang, Z., Liu, C. Q., Kawamura, K., Jiang, G., Shiraiwa, M., and Fu, P.: Increase of high molecular weight organosulfate with intensifying urban air pollution in the megacity Beijing, *J. Geophys. Res.-Atmos.*, **125**, e2019JD032200, <https://doi.org/10.1029/2019jd032200>, 2020b.
- Zhang, X., Lambe, A. T., Upshur, M. A., Brooks, W. A., Gray Be, A., Thomson, R. J., Geiger, F. M., Surratt, J. D., Zhang, Z., Gold, A., Graf, S., Cubison, M. J., Groessl, M., Jayne, J. T., Worsnop, D. R., and Canagaratna, M. R.: Highly oxygenated multifunctional compounds in α -pinene secondary organic aerosol, *Environ. Sci. Technol.*, **51**, 5932-5940, <https://doi.org/10.1021/acs.est.6b06588>, 2017.
- 920 Zhang, Y., Wang, K., Tong, H., Huang, R. J., and Hoffmann, T.: The maximum carbonyl ratio (MCR) as a new index for the structural classification of secondary organic aerosol components, *Rapid Commun. Mass Sp.*, **35**, e9113, <https://doi.org/10.1002/rcm.9113>, 2021.
- Zhao, D. F., Kaminski, M., Schlag, P., Fuchs, H., Acir, I. H., Bohn, B., Häseler, R., Kiendler-Scharr, A., Rohrer, F., Tillmann, R., Wang, M. J., Wegener, R., Wildt, J., Wahner, A., and Mentel, T. F.: Secondary organic aerosol formation from hydroxyl radical oxidation and ozonolysis of monoterpenes, *Atmos. Chem. Phys.*, **15**, 991-1012, <https://doi.org/10.5194/acp-15-991-2015>, 2015.
- 925

Formatted: Font color: Blue

Formatted: Font color: Blue

Formatted: Font color: Blue

Formatted: Font color: Blue

Formatted: Font color: Blue

Formatted: Font color: Blue

Formatted: Font color: Blue

Formatted: Font color: Blue

Formatted: Font color: Blue

Formatted: Font color: Blue

Formatted: EndNote Bibliography

Table 1. The chemical characteristics of β -pinene SOA and limonene SOA samples.

[O ₃] / ppbs	MW	O	O/C	DBE	OS _C	Volatility fractions (%)				
						ULVOCs	ELVOCs	LVOCs	SVOCs	IVOCs
β -Pinene SOA										
50	305	4.77	0.30	4.69	-0.98	14	28	33	17	8
315	307	5.49	0.35	4.40	-0.89	24	23	28	17	8
565	319	5.93	0.37	4.54	-0.84	30	23	23	16	8
Limonene SOA										
50	326	6.07	0.36	4.78	-0.82	12	21	30	25	12
315	349	6.88	0.39	4.99	-0.76	26	21	22	21	10
565	339	6.58	0.38	4.87	-0.78	26	21	23	20	10

Formatted: Line spacing: single

Formatted: Left, Space After: 0 pt

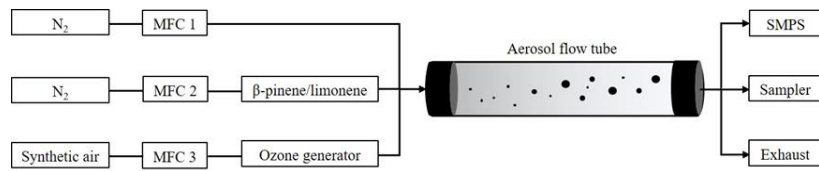
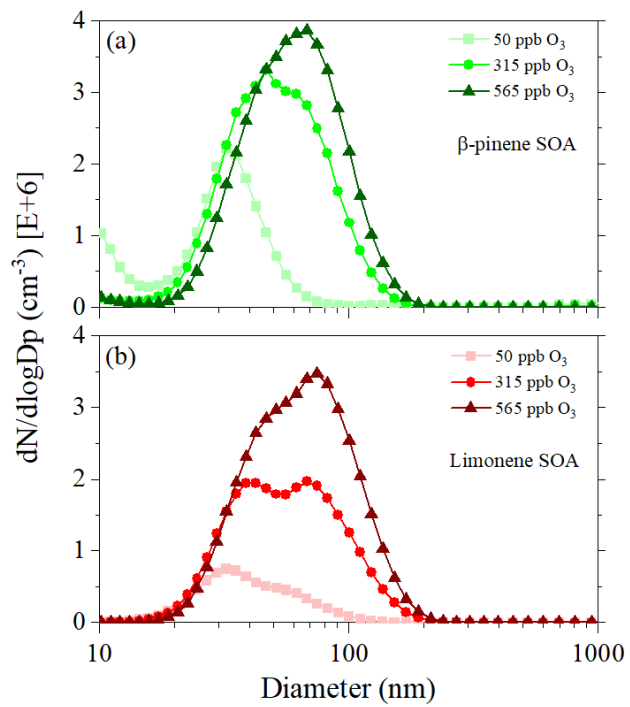


Figure 1. Schematic of the experimental setup for generation and collection of SOA. MFC: mass flow controller. SMPS: scanning mobility particle sizer.

935



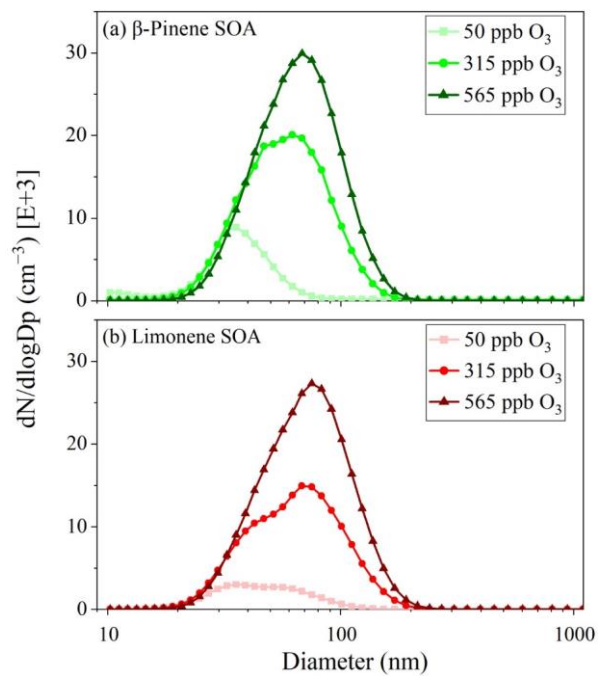


Figure 2. Particle size and number concentration distributions of the apparent particle sizes of β -pinene SOA (a) and limonene SOA (b) from as measured by SMPS measurement of β -pinene SOA (a) and limonene SOA (b).

940

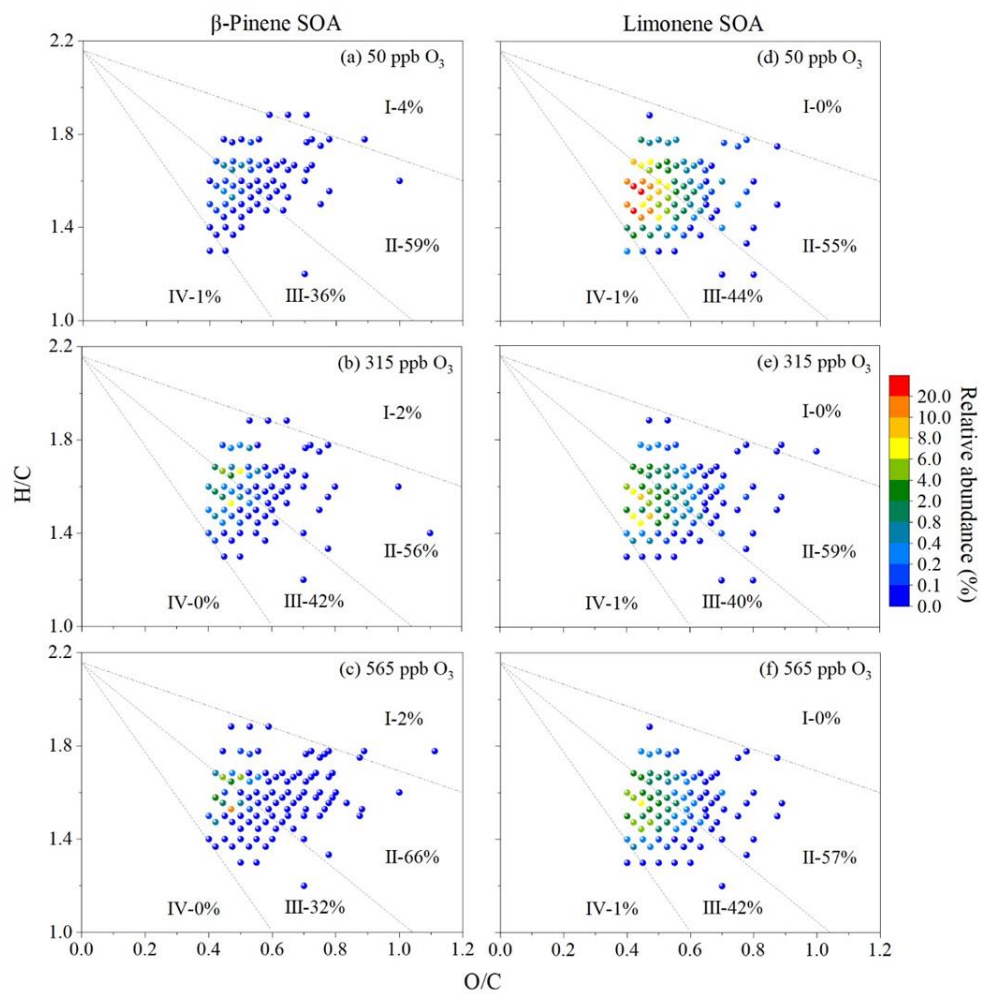
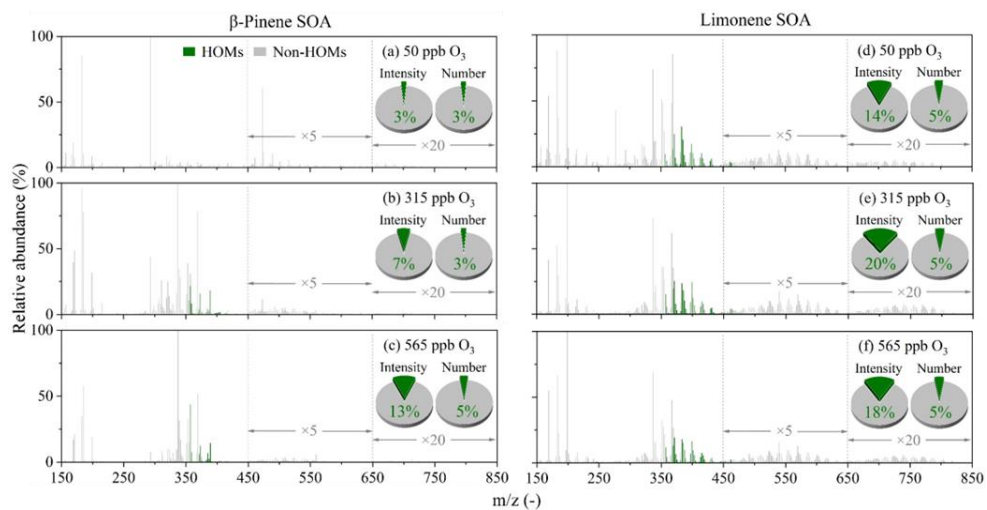
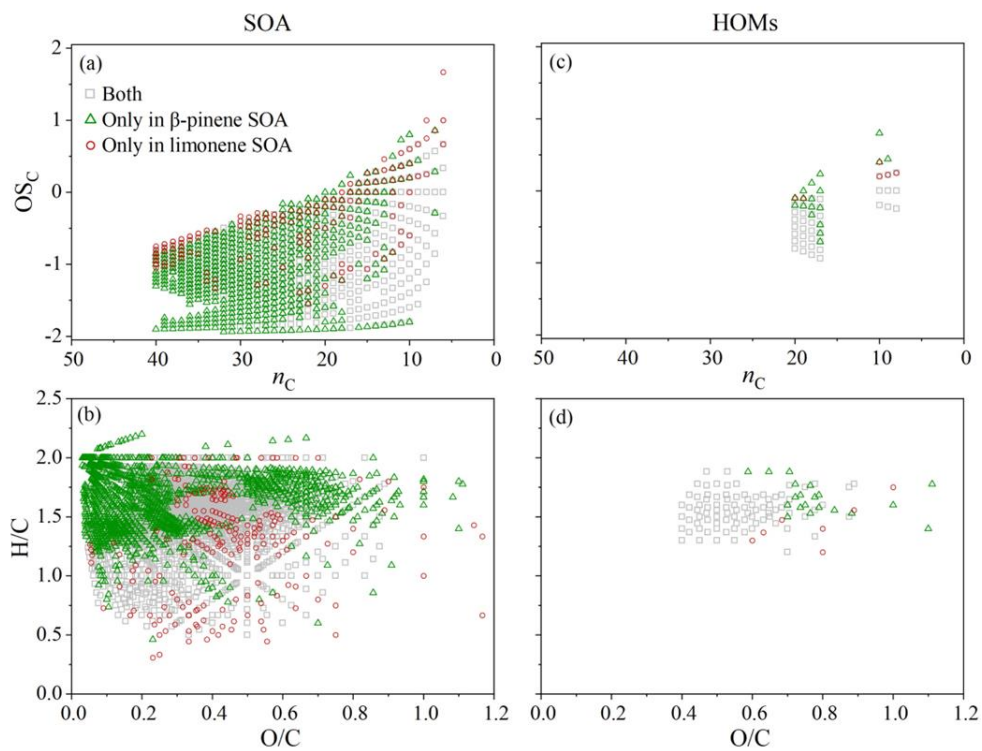


Figure 3. MCR-VK diagrams of β -pinene SOA (a, b, c) and limonene SOA (d, e, f) that formed at different ozone concentrations. The colors of the dots indicate the relative abundances of compounds.



945

Figure 4. Mass spectral fingerprint and relative abundances of HOMs (green) and non-HOMs (gray) in β -pinene SOA (a, b, c) and limonene SOA (d, e, f) that formed at different concentrations of ozone. The relative abundances of compounds with m/z 450–650 and 650–850 were increased by factors of 5 and 20, respectively. The pie charts indicate the ion intensity- and ion number- based relative abundances of different compounds.



950

Figure 5. The carbon oxidation state (OS_C) vs. the number of C atoms (n_C) (a, c) and Van Krevelen diagrams (b, d) for the unique assigned formulas from β -pinene SOA and limonene SOA and the corresponding HOMs (c, d). Gray squares represent assigned formulas observed both in β -pinene SOA and limonene SOA. Green triangles and red circles represent assigned formulas observed only in β -pinene SOA and limonene SOA, respectively.

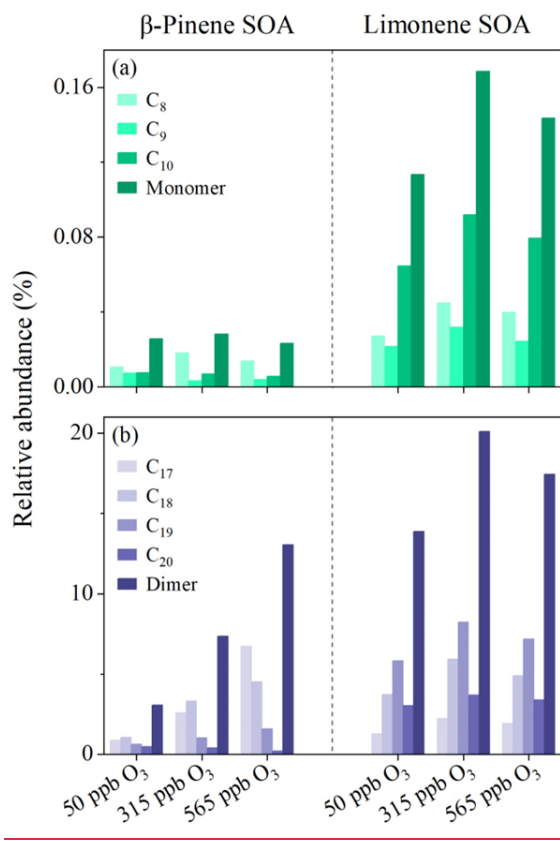
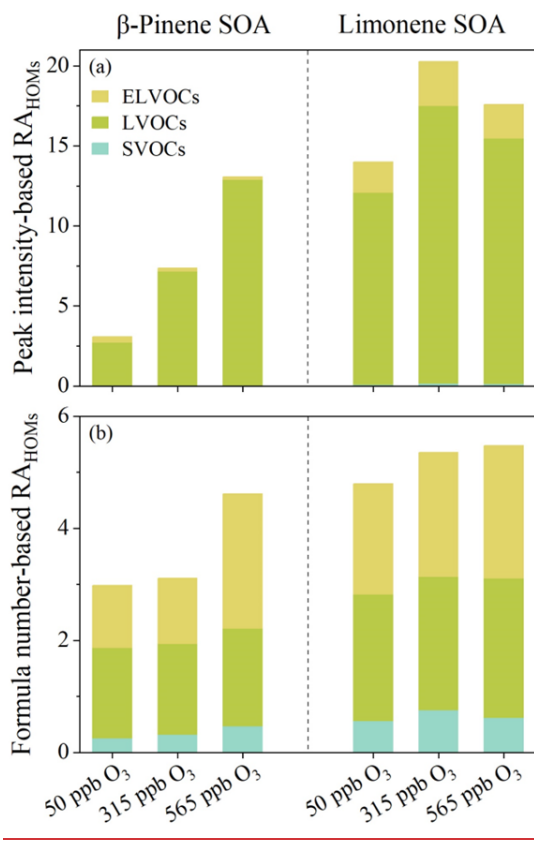
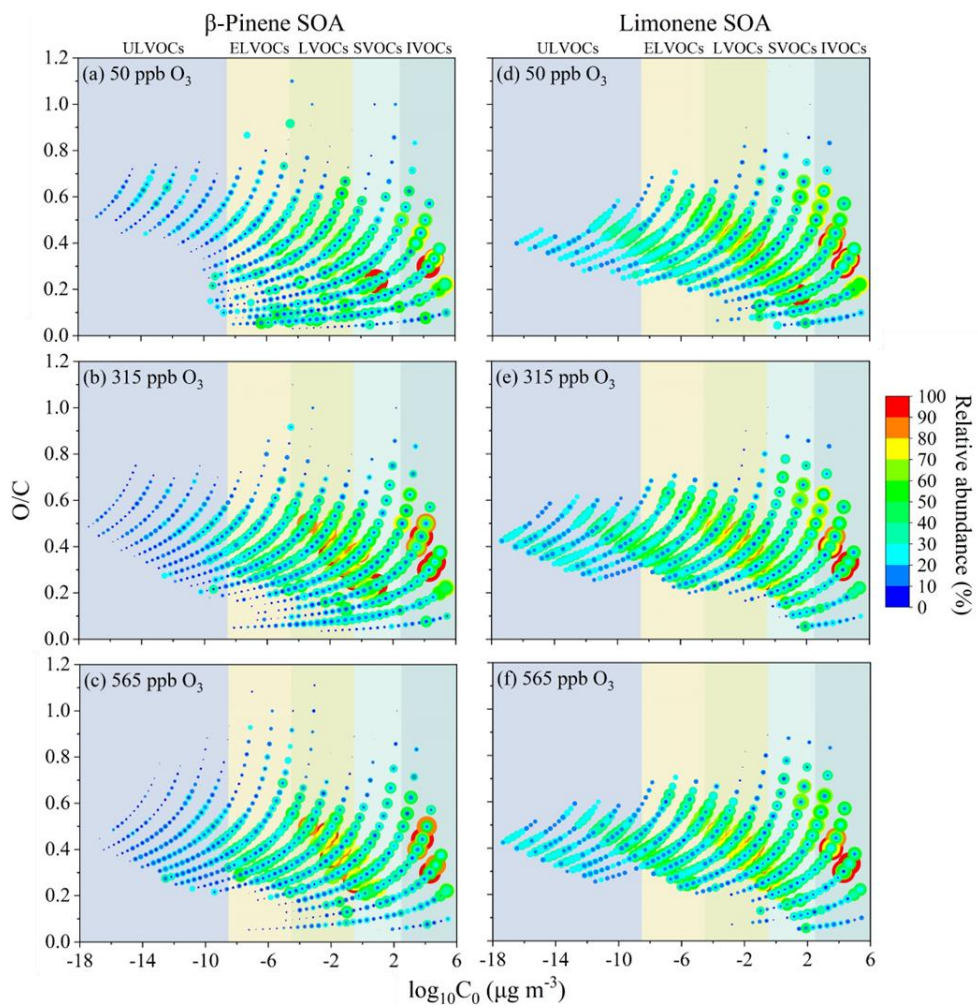


Figure 6. The relative abundance of HOMs monomers (a) and dimers (b) identified in β -pinene and limonene SOA as a function of carbon number (C_n).



960 **Figure 7.** The peak intensity- (a) and formula number- (b) based relative abundance of HOMs with different volatilities in SOA particles produced from ozonolysis of β -pinene and limonene under the three ozone concentrations.



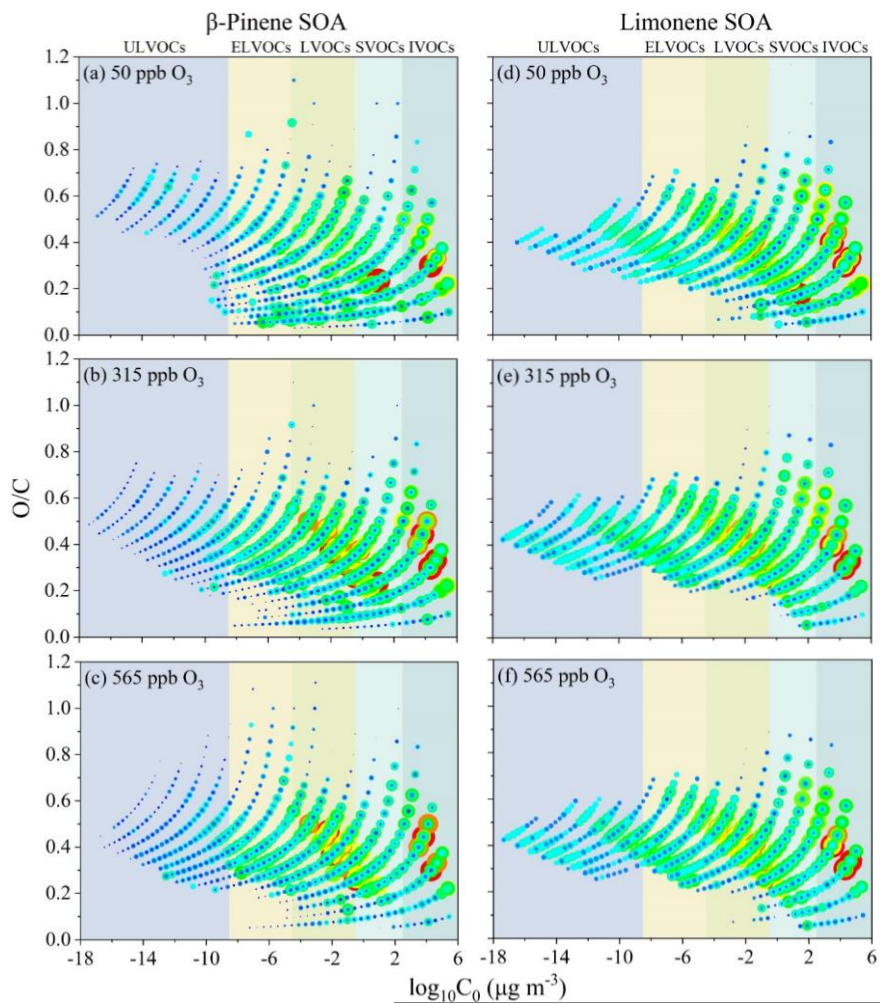


Figure 8. The pure compound saturation mass concentration (C_0) and the atomic oxygen and carbon ratios (O/C) of β -pinene SOA (a, b, c) and limonene SOA (d, e, f). Markers are color-coded and the dot size is scaled to the logarithm of relative abundance. The colour-coded color-codes and the size of the dots represent the relative abundance on a logarithmic scale.

Formatted: Font: Not Italic

Formatted: Font color: Blue

Formatted: Font color: Blue

Formatted: Font color: Blue

Formatted: Font color: Blue

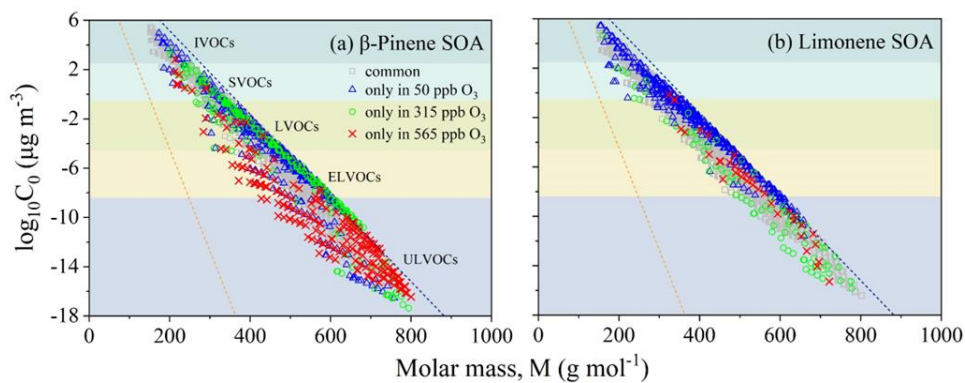


Figure 9. Molecular corridors of β -pinene (a) and limonene SOA (b) formed at 50 ppb, 315 ppb and 565 ppb ozone conditions. The gray squares represent the common compounds identified in SOA formed at three different ozone concentrations. The blue triangles, green circles, and red crosses indicate compounds only found in 50, 315, and 565 ppb ozone, respectively. The dotted lines represent linear n -alkanes $\text{C}_n\text{H}_{2n+2}$ (blue with $\text{O}/\text{C} = 0$) and sugar alcohols $\text{C}_n\text{H}_{2n+2}\text{O}_n$ (orange with $\text{O}/\text{C} = 1$).

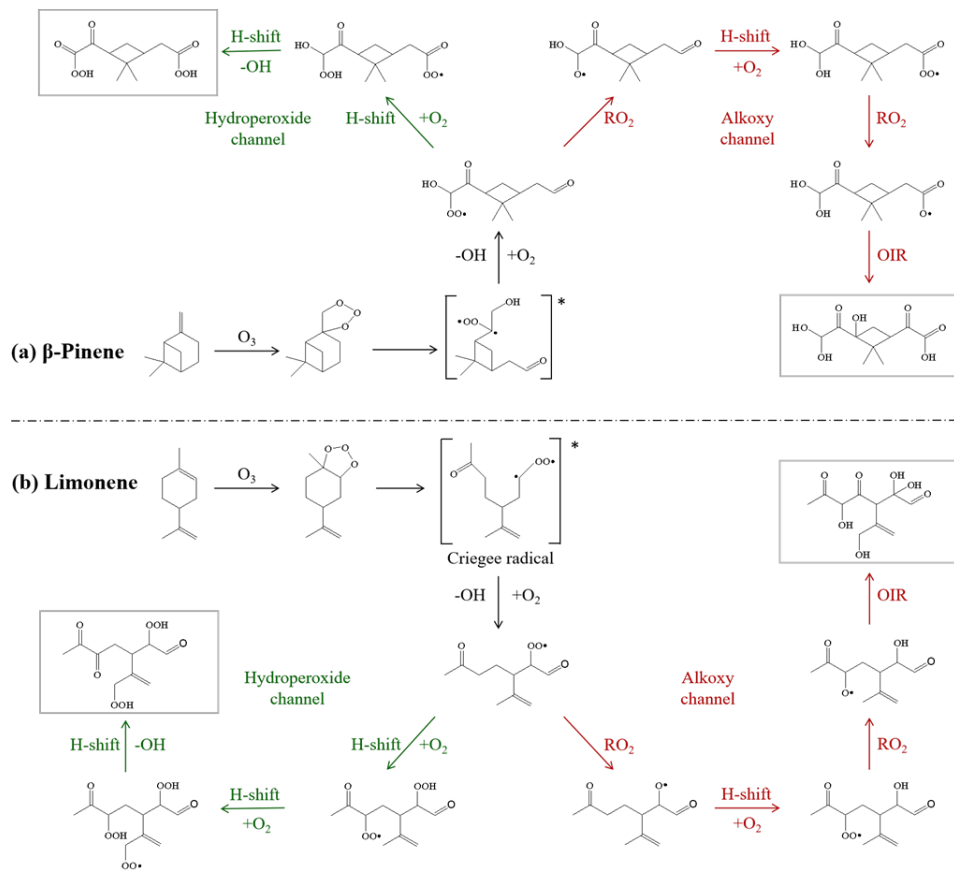


Figure 10. Proposed formation mechanism of C_{10} HOMs from the β -pinene and limonene ozonolysis via hydroperoxide channel (green) and oxygen-increasing reactions (OIR) (H-shift \rightarrow O_2 \rightarrow RO_2) of Criegee alkoxy channel (red) (Tomaz et al., 2021; Shen et al., 2021; Kundu et al., 2012). The $C_{10}H_{14}O_7$ organic molecules in the gray rectangle are the hypothesized structures.

Formatted: Left

Formatted: Font color: Blue

Formatted: Font color: Blue

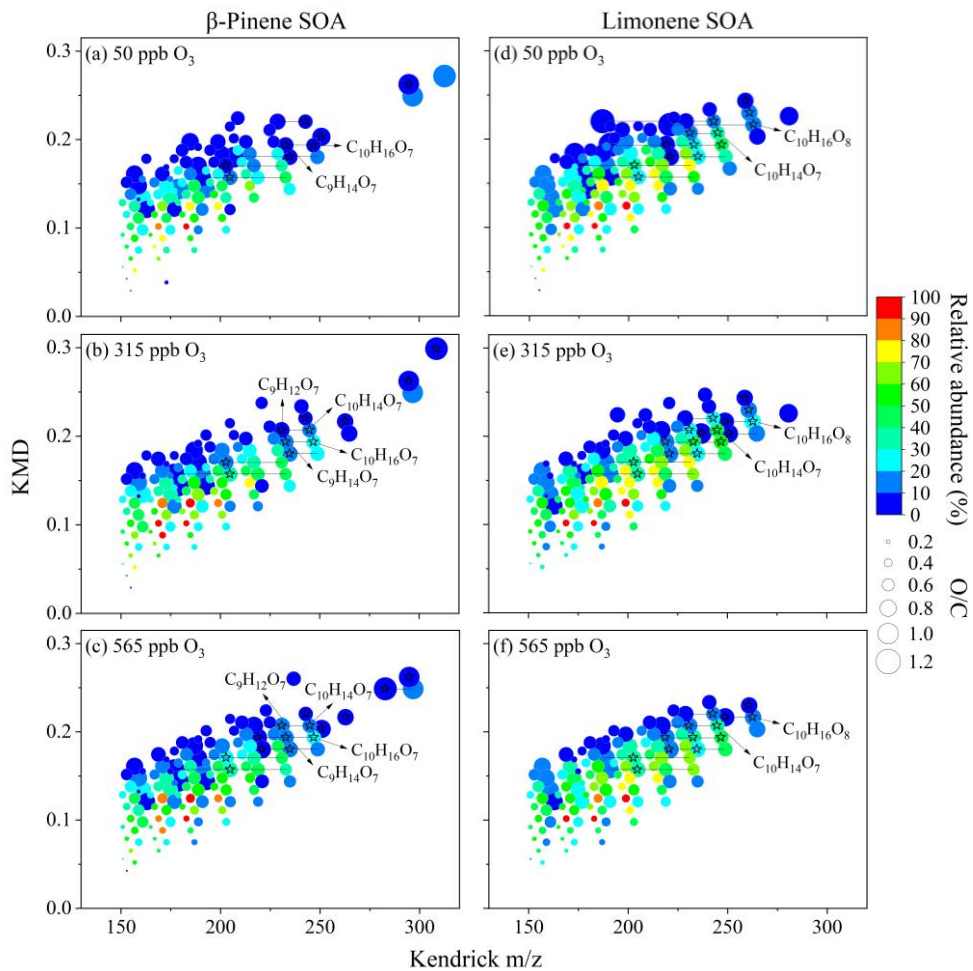


Figure 11. Kendrick mass defect of detected organic compounds in β -pinene SOA (a, b, c) and limonene SOA (d, e, f). Different colors represent the logarithm of relative abundance. Different dot sizes denote the atomic ratio of oxygen to carbon (O/C). The black pentagrams denote HOMs.